Modeling organic transformations by microorganisms of soils in six contrasting ecosystems: Validation of the MOMOS model

M. Pansu,[1] L. Sarmiento,[2] M. A. Rujano,[3] M. Ablan,[3] D. Acevedo,[2] and P. Bottner[4,5]

Received 26 March 2009; revised 31 August 2009; accepted 11 September 2009; published 26 February 2010.

[1] The Modeling Organic Transformations by Microorganisms of Soils (MOMOS) model simulates the growth, respiration, and mortality of soil microorganisms as main drivers of the mineralization and humification processes of organic substrates. Originally built and calibrated using data from two high-altitude sites, the model is now validated with data from a ^{14}C experiment carried out in six contrasting tropical ecosystems covering a large gradient of temperature, rainfall, vegetation, and soil types from 65 to 3968 m asl. MOMOS enabled prediction of a greater number of variables using a lower number of parameter values than for predictions previously published on this experiment. The measured ^{14}C mineralization and transfer into microbial biomass (MB) and humified compartments were accurately modeled using (1) temperature and moisture response functions to daily adjust the model responses to weather conditions and (2) optimization of only one parameter, the respiration rate k_{resp} of soil microorganisms at optimal temperature and moisture. This validates the parameterization and hypotheses of the previous calibration experiment. Climate and microbial respiratory activity, related to soil properties, appear as the main factors that regulate the C cycle. The k_{resp} rate was found to be negatively related to the fine textural fraction of soil and positively related to soil pH, allowing the proposition of two transfer functions that can be helpful to generalize MOMOS application at regional or global scale.

Citation: Pansu, M., L. Sarmiento, M. A. Rujano, M. Ablan, D. Acevedo, and P. Bottner (2010), Modeling organic transformations by microorganisms of soils in six contrasting ecosystems: Validation of the MOMOS model, *Global Biogeochem. Cycles*, *24*, GB1008, doi:10.1029/2009GB003527.

1. Introduction

[2] During the last decades, more than two hundred models have been proposed to predict biogeochemical transformations of carbon (C) and nitrogen (N) in soils [*Manzoni and Porporato*, 2009] and several times submitted to comparisons in terms of accuracy, structure, and hypothesis [e.g., *Smith et al.*, 1997; *Ma and Shaffer*, 2001; *McGechan and Wu*, 2001]. For agronomic purposes the modeling goal was to improve nutrient availability for plants without reduction of their soil storage especially in organic phase. For environmental and health preservation the aim was to predict carbon and nutrient transfer into groundwater and atmosphere. Most of organic transformations in soil are known to originate from energetic or metabolic activities related to microbial growth, maintenance, and byproducts (microbial cadavers and metabolites). However, surprisingly, most of the proposed soil organic matter (SOM) models use linear modeling approaches which do not explicitly include the specific functions of microorganisms in equations of the decomposition process. Some reviewed approaches [*Manzoni and Porporato*, 2007; *Wutzler and Reichstein*, 2008] consider both substrate and microbial biomass (MB) concentration in equations of Monod, Lotka-Volterra, or Michaelis-Menten type, which could agree with the observation of *Corstanje and Lark* [2008]: very few, if any, interesting soil models are strictly linear. *Pansu et al.* [2004] used data for a ^{14}C and ^{15}N tracer experiment to compare five alternative models, including Roth-C [*Jenkinson*, 1990], built on different hypotheses, and concluded that the best was to consider MB at the center of the decomposition process, proposing the new model, Modeling Organic Transformations by Microorganisms of Soil/Microorganismes et Matière Organique du Sol (MOMOS). MOMOS introduced a term of nonlinearity limited to the equation of MB respiration, while the other equations remained first-order functions describing (1) MB growth by ingestion of labile and stable materials of plant and microbial origin and (2) humification processes beginning by microbial mortality and progressing

[1] IRD, UMR Eco&Sols, INRA, CIRAD, SupAgro, Université Montpellier, Montpellier, France.
[2] ICAE, Facultad de Ciencias, Universidad de Los Andes, Mérida, Venezuela.
[3] CESIMO, Facultad de Ingeniería, Universidad de Los Andes, Mérida, Venezuela.
[4] CEFE, CNRS, Université Montpellier, Montpellier, France.
[5] Deceased 15 October 2006.

0886-6236/10/2009GB003527$12.00

Table 1. Characteristics of the Studied Sites

	El Vigia A(65)	Barinas A(165)	Tovar A(780)	Merida A(1800)	Gavidia A(3400)	El Banco A(3968)
			Site Characteristics			
Altitude (m)	65	165	780	1800	3450	3940
Latitude (°N)	8°37′33″	8°36′55″	8°20′32″	8°37′39″	8°40′04″	8°48′52″
Longitude (°W)	71°40′6″	70°12′15″	71°43′39″	71°9′17″	70°54′58″	70°55′30″
Typical ecosystem	tropical rain forest	natural savannah	seasonal forest	cloudy forest	paramo	high paramo
Actual vegetation	managed grassland	natural savannah	managed grassland	managed grassland	20 year fallow	natural paramo
Temperature[a]	27.4	26.4	23.0	17.4	8.9	5.5
Precipitation[b]	1825	1565	1112	1992	1338	790
AET[b]	1711	1297	1054	785	557	515
			Soil Characteristics			
WRB type[c]	Inceptisol	Alfisol	Mollisol	Inceptisol	Inceptisol	Entisol
C g kg^{-1}	36.77	13.67	48.23	102.27	100.57	61.53
N g kg^{-1}	2.80	0.90	3.70	6.10	5.27	2.77
C:N	13.1	15.2	13.0	16.8	19.1	22.2
pH_{water}	5.1	5.7	6.1	5.2	4.6	4.7
CEC[d]	13.9	5.2	13.1	26.5	24.8	12.1
Sand (%DW)	67.3	77.0	62.0	69.3	40.0	62.0
Silt (%DW)	24.0	14.0	31.3	25.3	42.0	30.0
Clay (%DW)	8.7	9.0	6.7	5.3	18.0	8.0
WHC[e]	37.82	14.69	21.38	37.71	35.67	21.42
WCWP[e]	16.29	2.33	4.78	29.68	18.09	7.10
WCI[e]	27	8.5	13	33	26	14

[a]Long-term annual mean temperature in °C.
[b]Long-term annual mean precipitation and evapotranspiration (mm).
[c]*FAO, UNESCO, and ISRIC* [1988].
[d]CEC, Cation Exchange Capacity mmol (+) kg^{-1}.
[e]WHC, Water Holding Capacity; WCWP, Water Content at Wilting Point; and WCI, Water Content Initial in soil bags (% DW).

by slow chemical maturation of fresh humus. Thus microbial respiration was found to be an essential term driving microbial dynamics more in accordance with data than the previous model propositions. Another MOMOS innovation was to eliminate the parameters concerning C utilization efficiency or partitioning coefficients (*r* in the work of *Manzoni and Porporato* [2009]). Literature data generally attribute constant values to *r* and do not mention links between *r* and environmental variables, but predictions were found sensitive (Monte Carlo simulations) to little changes in the value of these *r* constants [*Pansu et al.*, 2004]. Thus, the MOMOS parameters are only rate constants bond to the quality of organic inputs [*Bottner et al.*, 2006], soil texture [*Pansu et al.*, 2007], temperature, and moisture conditions, making the model probably the most sensitive to climate change.

[3] Since MOMOS was originally calibrated from a tracer experiment carried out in two high mountain sites of Bolivia and Venezuela, the first aim of this study was to validate the model and associated hypotheses in a much larger range of climate and soil conditions. The validation data came from the previous Transalt experiment where the same standard labeled material was buried in six contrasting sites of Venezuela which represented probably the largest altitudinal gradient used in a tracer experiment (65 to 3968 m). Soil moisture, total ^{14}C, and MB-^{14}C were periodically measured during more than 3 years in the labeled samples. In a previous publication, *Coûteaux et al.* [2002] evaluated the mineralization dynamics by means of adjusting double exponential equations to the total ^{14}C data of Transalt, previously corrected by temperature and moisture response functions. Eighteen parameter values were necessary to describe ^{14}C mineralization along the gradient, and only 30% of the between-site variability could be ascribed to climatic differences. *Braakhekke and de Bruijn* [2007] reanalyzed the same data to reduce the modeling complexity but had to maintain different mineralization rates for each site, and 13 parameter values were again necessary to predict the whole total ^{14}C data. The Transalt data were never used before to predict the ^{14}C transfer processes both in humus and atmosphere and validate models of organic matter in soil. Additionally to MOMOS validation, this modeling exercise aimed to better understand the respective role of temperature, moisture, and soil properties on microbial functioning acting on C mineralization or sequestration. Finally, this work attempted to improve equations relating the microbial respiration to soil properties as a tool to scale up MOMOS results at regional level and potentially improve global change predictions.

2. Materials and Methods

2.1. Experimental Sites

[4] The Transalt experiment was carried out in six sites along an altitudinal transect in Venezuela, from 65 to 3968 m above sea level (asl), covering a large bioclimatic gradient that includes (1) tropical rain forest, (2) seasonal savanna, (3) seasonal montane forest, (4) cloud forest, and (5) Andean paramo (alpine vegetation) at two elevations. Table 1 presents the sites, their abbreviations, and their climatic and soil characteristics.

[5] The lowest site of the transect, A(65), situated at 65 m asl, west of the Andes and near the city of El Vigia, is characterized by a tropical rain forest climate without a pronounced dry season (Figure 3a). The original vegetation has

been deforested, and the area is now intensively used for cattle raising and agriculture. The study plot was located in a managed grassland dominated by the African grass *Brachyaria humidicola*. The soil is an Inceptisol [*Food and Agriculture Organization, United Nations Educational, Scientific and Cultural Organization, and International Soil Reference and Information Centre* (*FAO, UNESCO, and ISRIC*), 1988] and contained 67% sand; it was the most acid of the low-altitude sites, and its water holding capacity was the greatest of the six sites and similar to those of the two other mountain Inceptisols of Merida and Gavidia. Its organic content was lower but more nitrogenous than that of the mountain sites (Table 1).

[6] The other low-altitude site, A(165), was situated in the city of Barinas, at 165 m asl, on the opposite east flank of the Andes. It was characterized by a typical seasonal savanna climate with a pronounced dry season of 4–5 months where soil water of the surface layers stays below the permanent wilting point (Figure 4a). The experimental plot was situated on the natural savanna dominated by perennial tussocks (*Axonopus purpusii*, *Leptocoryphium lanatum* and *Trachypogon vestitus*) and isolated trees. The soil is an Alfisol, which contained the greatest amount of sand, the lowest amount of C, and had the lowest water holding capacity of the six sites (Table 1).

[7] The seasonal montane forest site, A(780), was situated in an inner Andean valley, close to the city of Tovar, at 780 m asl, with a lower annual rainfall than the previous sites and three dry months (Figure 5a). The native vegetation, dominated by deciduous trees, was almost completely transformed to coffee plantations and managed grasslands. The study plot was situated in a secondary grassland on a Mollisol, which was the less acid of the transect, with 38% of 0–20 μm fine fraction and near 5% organic C, and other soil characteristics that were intermediary between soils of the low altitude sites and those of higher mountains, and a C:N ratio similar to that of the fertile A(65) site (Table 1).

[8] The Merida site, A(1800), was situated at the lower limit of the cloud forest, at 1800 m asl, and is characterized by the highest precipitation of the transect, without a pronounced dry period (Figure 6a), high cloudiness together with fogs, mist, low radiation, and a high relative air humidity. The study plot was situated on a secondary grassland dominated by the African grass *Melinis minutiflora*. The soil organic matter content of this Inceptisol was, together with the soil of Gavidia, the highest of the experimental sites, with slightly more nitrogen in Mérida. This soil was also the most fertile in terms of cation exchange capacity, although its sandy texture was similar to that of A(65), indicating probably a higher contribution of the soil organic matter. The water holding capacity was high and similar to that of A(65) and A(3400) soils.

[9] The Andean paramo site of Gavidia, A(3400), was located in a glacial valley at 3400 m asl, near the upper limit of agriculture. The mean temperature is 8.9°C with large daily fluctuations including night frosts occurring mainly in the dry season from November to March (Figure 7a). The paramo vegetation is dominated by the typical giant rosettes of *Espeletia schultzii*, several species of shrubs (*Hypericum laricoides*, *Baccharis prunifolia*, *Acaena elongata*, *Stevia lucida*), and grasses (*Calamagrostris effusa*, *Bromus carinatum*, *Nasella mucronata* and *Trisetum irazuense*). The study plot was situated in an old fallow field on a humic Inceptisol having the finest texture and the lowest pH of the experimental sites, conjointly with good production capacities in terms of water holding and cation exchange.

[10] The highest site of El Banco, A(3968), situated at 3968 m asl, is under the influence of a high-altitude tropical climate with a mean temperature of 5.5°C, with pronounced daily fluctuations including frequent night frosts throughout the year. The annual precipitation of only 790 mm was the lowest of the transect and was characterized by dry period of 4 months (Figure 8a). Giant rosettes of *Espeletia schulttzii* and shrubs of *Hypericum laricoides* dominate the vegetation. N content, cation exchange capacity, and water holding capacities were lower than in the other mountain sites.

[11] All together, this altitudinal transect is characterized by contrasting conditions of temperature, annual precipitation, seasonal distribution, and soil characteristics. The long-term mean annual air temperature ranged from 5.5°C in A(3968) to 27.4°C in A(65), and the mean annual precipitation ranged from 790 in A(3968) to 1992 mm in A(1800). The soils were differentiated in terms of their carbon content in the 0–10 cm layer, going from 13 in A(165) to more than 100 g (C) kg^{-1} (soil) in A(1800) and A(3400). The quality of the soil organic matter was also different along the transect with C:N ratios ranged from 13 in A(65) and A(780) to 15 in the savanna site A(165) and increased from 17 to 22 at the highest sites A (1800) to A(3968). Soils were acid in all sites but mainly in the two paramo soils. Textural characteristics (Table 1) showed a loam soil on site A(3400) and sandy loam soils on the other sites. The savanna soil of site A(165) contained the highest amount of sand and the lowest amounts or organic matter; both its capacities of water holding and cation exchange were the lowest of the studied sites. Inversely, the mountain soils A(1800) and A(3400) contained the highest amounts of fine particles and organic matter and showed the highest capacities of both water holding and cation exchange. The three other soils were intermediary both in capacities of water holding and cation exchange.

2.2. Experimental Design and Data Collection

[12] The experimental plots were placed either in natural herbaceous vegetation in the savanna and paramo sites or in managed grassland in the forests sites to minimize the variability due to the effect of vegetation on microclimate conditions, mainly on soil temperature. A standard plant material was decomposed in 14 × 15 cm soil bags containing soil from the top 0–10 cm layer of the different sites. The soil weight per bag was calculated to reproduce the natural bulk density with a volume of 210 cm^3. The top part of the bags had a 1 mm mesh to allow the access of plant roots and mesofauna, and the mesh of the bottom part was 0.1 mm to minimize losses by gravity. A standard wheat straw with high ^{14}C activity was mixed to the soil. It was obtained from cropping the wheat in a labeling chamber controlled for temperature, radiation, moisture, and CO_2 concentration. The wheat was grown from seed to maturity for 4 months under a ^{14}C labeled atmosphere and on a NPK+micro-nutrients solution. The straw contained 39.44% C with a specific activity of 0.875 kBq mg C^{-1}. It was roughly ground to <5 mm particles.

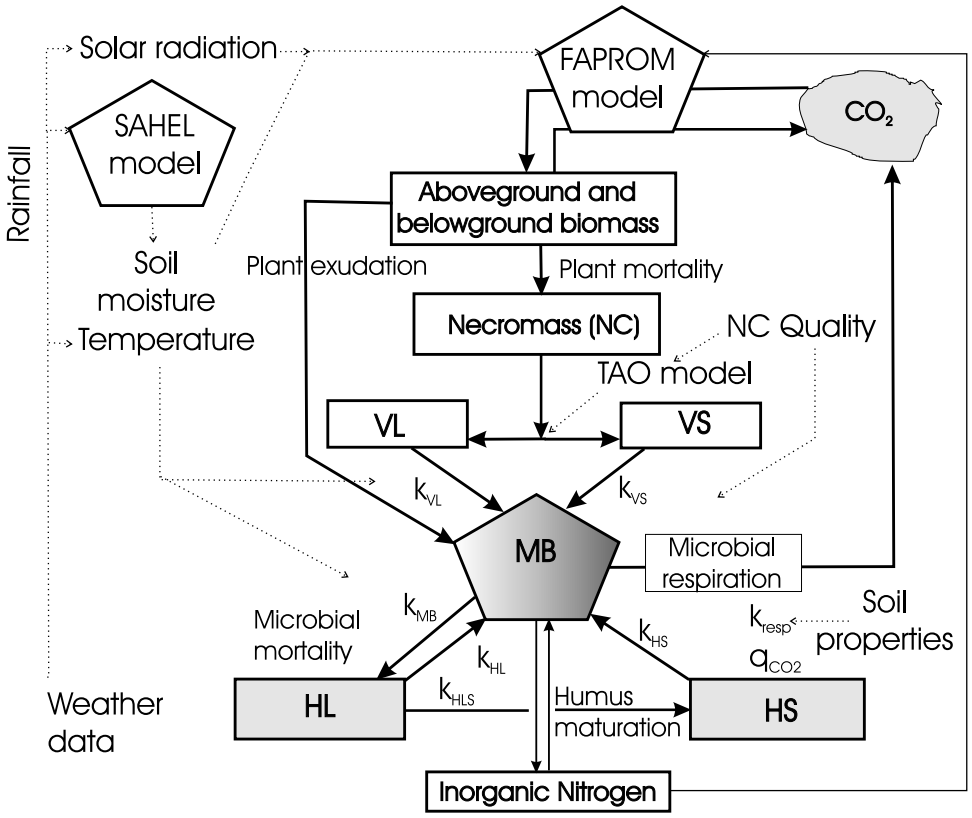

Figure 1. Relational diagram of the Modeling Organic Transformations by Microorganisms of Soils (MOMOS) model here coupled with the soil water model SAHEL and the fallow production model FAPROM [*Pansu et al.*, 2009]. NC, VL, and VS are total, labile, and stable necromass, respectively; MB is microbial biomass; HL is labile humus; HS is stable humus; k_{VL}, k_{VS}, k_{HL}, and k_{HS} are rates of microbial assimilation of VL, VS, HL, and HS, respectively; qCO_2 is metabolic quotient of MB, $C°_{BM}$ is basal MB at steady state, k_{resp} is respiration rate of MB, k_{MB} is mortality rate of MB, and k_{HLS} is maturation rate of humus. Split of NC into VL and VS is regulated by the Transformation of Added Organic Materials (TAO) model [*Thuriès et al.*, 2002].

The added plant material carbon ranged from 1.4 to 11.6% of the initial native C in the soil.

[13] A total of 40 soil bags containing the labeled straw were buried at 5 cm depth (10 sampling occasions × 4 replicates at each site, making a total of 240 soil bags). At installation (23 November to 6 December 1994), the soil bags were moistened with deionized water to put the initial water content at the middle of the available water capacity (Table 1). The soil bag exposure time ranged, depending on the altitude, from 18 months in the two lowest sites, to 24 in A(780), 31 in A(1800), and 38 months in the two highest sites. The first sampling took place 1 month after the installation, and the sampling interval increased with time to reach 6 months at the end of the experiment for the highest sites.

[14] The ^{14}C total carbon concentration in the original straw and in the labeled soil bags was determined on four replicates using dry combustion (Carmhograph 12A carbon analyzer, Wosthoff, Bochum, Germany) and liquid scintillation counting [*Bottner and Warembourg*, 1976]. The calculated number of disintegrations per minute (DPM) was divided by the corresponding value of the labeled straw at the beginning of incubation to obtain the fraction of the added labeled material still remaining in the soil. The ^{14}C-BM was determined using the fumigation-extraction method [*Brookes et al.*, 1985]. After sampling, the soil bags were maintained refrigerated for no more that a few days before the analysis was performed. After homogenization, a fresh soil sample equivalent of 30 g dry soil was fumigated with alcohol-free chloroform for 18 h. The fumigated and an equivalent control soil sample were extracted with 150 ml of K_2SO_4 0.5 M for 30 min and centrifuged. The radioactivity was measured by duplicate in each fumigated and control extract using liquid scintillation counting. The ^{14}C-BM was calculated as the difference between the dpm of the fumigated and control extracts, corrected using a Kc factor of 0.45 [*Joergensen*, 1996], and divided by the specific activity of the straw.

[15] Soil moisture of the soil was estimated in each soil bag using four replicates of 5 g that were dried at 105°C for 24 h. Other soil analyses were performed according to the standard methods [*Pansu et al.*, 2007].

2.3. Decomposition Model MOMOS

[16] MOMOS (Figure 1) is a five-compartment model centered on the activity of soil microbial biomass (MB) that

grows by ingestion of labile (VL) and stable (VS) plant materials as well as labile (HL) and stable (HS) humus and decreases by microbial respiration and mortality [*Pansu et al.*, 2004, 2007; *Bottner et al.*, 2006]. The only process which is assumed to be more physicochemical than biological is humus maturation from HL to HS. MOMOS is parameterized only by seven first-order rate constants (dimension is d^{-1}) and does not use partitioning coefficients as many other soil organic matter models do. All MOMOS parameters are constrained by soil moisture and temperature using response functions ranging from 0 to 1, resulting in high sensitivity to climate change as shown in the general MOMOS equation:

$$\dot{\mathbf{x}} = f(T)f(\theta)\ \mathbf{A}\ \mathbf{x} + \mathbf{B} \tag{1}$$

where $\mathbf{x}$ is the vector of the state variables (^{14}C content of compartments), $\dot{\mathbf{x}}$ is the corresponding vector of the rate variables, $\mathbf{A}$ is the parameter matrix of the model, $\mathbf{B}$ is a vector regulating the external C input by exudation and senescence originated from photosynthesis [*Pansu et al.*, 2009] (= 0 for labeled data), and $f(T)$ is the response function to temperature correction set to the exponential function (see section 4.2):

$$f(T) = Q_{10}^{(T-T_{opt})/10} \tag{2}$$

where T is the actual daily soil temperature (0–10 cm layer) set equal to air temperature; T_{opt} is the optimal decomposition temperature settled at 28°C, a temperature often used to perform laboratory decomposition experiments under optimal conditions [*Thuriès et al.*, 2001] and just above the mean annual temperature of the warmer sites A(65) and A(165) of this study; Q_{10} is the rate increase when T increase by 10°C finally fixed at 2.2 for all sites of this study (see section 4.2); and $f(\theta)$ is the response function to soil moisture expressed in fraction of WHC (Table 1; see section 4.2):

$$f(\theta) = \mathrm{MIN}\left(\frac{\theta}{WHC}, 1\right) \tag{3}$$

[17] The soil daily moisture θ was predicted using SAHEL [*Penning de Vries et al.*, 1989], a tipping bucket-type model that calculates daily values of soil moisture by layer using climate data (daily maximal and minimal temperature, precipitation, and latitude), soil data on water retention (Table 1), and plant cover as inputs. The model was calibrated for each site using the soil moisture measured in the soil bags, and then daily moisture data for the layer 0–10 was generated [*Pansu et al.*, 2004]. Meteorological data for the interval of the experiment were collected for each site from the nearest weather station. For A(65), A(165), and A(1800) there were available climate data for the study period coming from weather stations near the experimental plots. For A(780) and A(3400) there were weather stations near the plots but data were not available for the study period. In these two cases, monthly linear correlations between the available data of the closest weather station (for other periods) and those of other weather stations situated close to the study area were used to estimate monthly precipitation. Monthly estimates were transformed to daily values using a Markov transition probability matrix to model the probability of a precipitation on a given day and a gamma distribution for calculating the actual amount of precipitation. Both transition probability matrices and gamma parameters were estimated using daily historical data. Several runs were generated, and the one with the best agreement with the monthly values for the experiment time period was selected. For A(3968), the closest weather station was situated at an altitude 800 m below the experimental site, so weather data were corrected by altitude (considering a decline of 0.6°C each 100 m) and by a factor of 1.26 obtained from a isohyets map of the rainfall.

[18] The model matrix $\mathbf{A}$ and vector $\mathbf{x}$ are

$$\mathbf{A} = \begin{bmatrix} -k_{\mathrm{VL}} & 0 & 0 & 0 & 0 \\ 0 & -k_{\mathrm{VS}} & 0 & 0 & 0 \\ k_{\mathrm{VL}} & k_{VS} & -(q_{CO_2} + k_{\mathrm{MB}}) & k_{\mathrm{HL}} & k_{\mathrm{HS}} \\ 0 & 0 & k_{\mathrm{MB}} & -(k_{\mathrm{HL}} + k_{\mathrm{HLS}}) & 0 \\ 0 & 0 & 0 & k_{\mathrm{HLS}} & -k_{\mathrm{HS}} \end{bmatrix} \text{ and } \mathbf{x} = \begin{bmatrix} x_{\mathrm{VL}} \\ x_{\mathrm{VS}} \\ x_{\mathrm{MB}} \\ x_{\mathrm{HL}} \\ x_{\mathrm{HS}} \end{bmatrix} \tag{4}$$

[19] At each incubation time, the total C decrease ($\dot{c}$ from the five compartments $i \in$ [VL, VS, MB, HL, HS]) is

$$\dot{c} = \sum_{i=1}^{5} \dot{x}_i = -q_{\mathrm{CO_2}} x_{\mathrm{MB}} \tag{5}$$

where $q_{\mathrm{CO_2}}$ is the metabolic quotient of the microbial biomass:

$$q_{\mathrm{CO_2}} = k_{resp} \frac{x_{MB}}{C^0_{\mathrm{MB}}} \tag{6}$$

where k_{resp} is the respiration coefficient, (dimension is d^{-1}) scaled by C^0_{MB}, the biomass at steady state (estimated on bare soil unsupplied with recent input of substrate, here estimated from the values of measured MB-^{14}C at the end of the incubation). If C_0 is the amount of initially added ^{14}C (= 1 for these data scaled by the ^{14}C input), and f_S its stable fraction, the initial conditions for the ^{14}C experiment were given by

$$x_{\mathrm{VL}}(0) = (1 - f_S)C_0,\ x_{\mathrm{VS}}(0) = f_S C_0,\ x_{\mathrm{MB}}(0) = 0,\ x_{\mathrm{HL}}(0) = 0,\ x_{\mathrm{HS}}(0) = 0 \tag{7}$$

[20] *Thuriès et al.* [2002] proposed the three-pool model TAO to predict specifically the transformation of added organic matters from laboratory incubation data. A similar three-pool model was proposed by *Adair et al.* [2008] to predict in situ litter mass losses. In this study the input part of MOMOS was simplified at two pools giving satisfying prediction accuracy. The stable fraction f_S was estimated as that of the stable TAO compartment using equations proposed by *Thuriès et al.* [2002] between f_S and biochemical composition of straw, which gave f_S = 0.14.

[21] The Powell optimization method was used to estimate the values of the microbial respiration rates k_{resp} for each soil

Table 2. Optimized Values of Microbial Respiration Rate and Statistical Tests of Predictions at Each Site and on the Whole Data Set

	El Vigia A(65)	Barinas A(165)	Tovar A(780)	Merida A(1800)	Gavidia A(3400)	El Banco A(3968)	Whole Data Set
C^0_{MB} [a]	0.0107	0.0106	0.0192	0.0129	0.0185	0.0156	
k_{resp} [b]	0.029	0.038	0.034	0.029	0.021	0.022	
Statistical Tests for Moisture Predictions							
F [c]	7.8***	132.8***	16.4***	24.7***	28.2***	12.3***	254.8***
$a \pm SE_a$ [d]	1.00 ± 0.09	0.97 ± 0.05	0.92 ± 0.10	0.97 ± 0.07	0.92 ± 0.05	1.04 ± 0.11	0.97 ± 0.03
Statistical Tests for MB-^{14}C Predictions							
F [c]	7.4**	6.7**	2.5 NS	11.2***	1.7 NS	2.8 NS	3.6***
$a \pm SE_a$ [d]	0.84 ± 0.03	0.94 ± 0.06	0.69 ± 0.02	0.98 ± 0.05	1.29 ± 0.05	1.20 ± 0.07	0.98 ± 0.03
Statistical Tests for Total-^{14}C Predictions							
F [c]	137.9***	27.8***	55.4***	66.7***	35.8***	11.9***	46.1***
$A \pm SE_a$ [d]	1.00 ± 0.01	0.98 ± 0.02	1.00 ± 0.02	1.00 ± 0.02	1.00 ± 0.01	0.99 ± 0.03	0.99 ± 0.01

[a]The ^{14}C-MB at steady state (equation (6)) in g MB-^{14}C g^{-1} added-^{14}C.
[b]Optimized value of microbial respiration rate (equation (6)) in d^{-1}.
[c]F test; see equation (9): ***, significant at 1% risk; **, significant at 2% risk; NS, not significant (5% risk).
[d]Slope a, equation (10); absence of bias if $a = 1$. SE_a = associated standard error.

of the six experimental sites. The values of the other MOMOS optimal parameters (for a temperature and moisture correction factor of 1) were used unchanged from the MOMOS previous calibration experiment [*Pansu et al.*, 2004, 2007]:

[22] microbial mortality rate k_{MB} 0.45 d^{-1},

[23] microbial ingestion rate of labile plant materials k_{VL} 0.6 d^{-1},

[24] microbial ingestion rate of stable plant materials k_{VS} 0.003 d^{-1},

[25] microbial ingestion rate of labile humus k_{HL} 0.05 d^{-1},

[26] microbial ingestion rate of stable humus k_{HS} 0.00005 d^{-1},

[27] maturation rate from labile humus to stable humus k_{HLS} 0.0003 d^{-1}.

[28] The microbial mortality rate (k_{MB}) represents not only the mortality sensu stricto but also the production of byproducts resulting from microbial metabolism. All these parameter values, as well as the optimized k_{resp} values (Table 2), represent maximal microbial activity in optimal conditions of temperature and soil moisture. They were daily reduced by the calculated value of the $f(T)f(\theta)$ response function (equation (1)) ranged in the 0–1 interval. The model was developed in VENSIM 5.6b (http://www.vensim.com).

2.4. Statistical Tests

[29] At each i of the p sampling occasions using $\alpha = 1 \ldots n$ ($n = 4$) replicates, the expected value y_i of water content, MB-, and Total-^{14}C associated to mean $\overline{y}_i$ and pooled confidence interval (plotted on Figures 3–8 for MB- and Total-^{14}C) was

$$\overline{y}_i \pm t^{n-1}_{0.975} \sqrt{\frac{1}{n(np-p)} \sum_{i=1}^{p} \sum_{\alpha=1}^{n} (y_{i\alpha} - \overline{y}_i)^2} \qquad (8)$$

[30] The significance of MOMOS predictions comparative to mean of measured values was tested by

$$F = \frac{\sum_{i=1}^{p} (\overline{y}_i - \overline{y})^2}{\sum_{i=1}^{p} (\overline{y}_i - \hat{y}_i)^2} \qquad (9)$$

where $\hat{y}_i$ is the MOMOS predicted value corresponding to y_i and $\overline{y}$ is the mean of the data series. Equation (9) gave F values of Table 2 which were compared to F tables for bilateral tests at 1%, 2%, and 5% risk. A complementary graphical comparison (Figures 3 to 8) enables us to show if predicted values are included or not in confidence intervals of equation (8).

[31] Another graphical comparison was used to plot predicted versus measured values using the linear regression model:

$$\hat{y}_i = (a \pm SE_a)\overline{y}_i \qquad (10)$$

where the slope a associated to its standard error SE_a enabled us to detect relative bias. No significant absolute bias was detected, so equation (10) assumed a zero value to the intercept point [*Pansu et al.*, 2001]. Test of equation (10) was first applied to the whole data series of moisture content and total-^{14}C. Results of test (10) on the whole data series are plotted on Figure 2. Test (10) was then applied site by site, giving the $a \pm SE_a$ results in Table 2.

3. Results

3.1. Weather Data, Moisture Prediction, and Climate Response Functions

[32] For all the sites, in accordance to the closeness to the equator, there were no marked seasonal trends in air temperature, and daily variations due to cloudiness were greater than the seasonal changes. However, the effect of altitude on temperature was very important and represents the most important driving factor controlling decomposition dynamics in this transect. The less reduction factors to temperature were calculated for the lowest sites (A(65) and A(165)), giving $f(T) \approx 1$ with oscillations between 0.7 and 1, then $f(T)$ between 0.65 and 0.9 for A(780), between 0.3 and 0.5 for A(1800), between 0.2 and 0.3 for A(3400), and between 0.15 and 0.2 for A(3968).

[33] Table 2 shows that SAHEL predictions of soil moisture agreed with the data measured in the soil bags. F test (equation (9)) was significant at $p = 0.01$ for the whole data set and also for each site taken individually. In all the cases, the

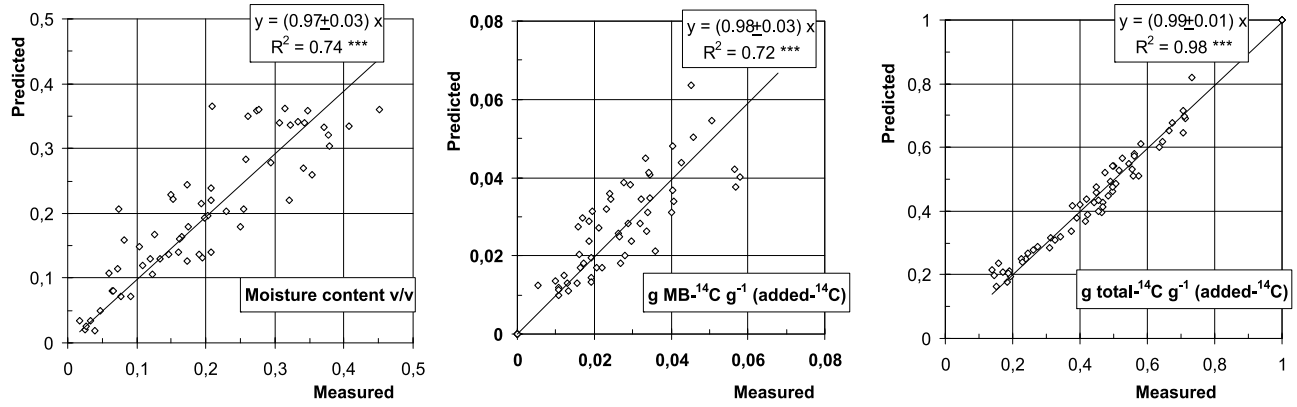

Figure 2. Relationships between predicted and measured (means of four replicates) values of (1) soil moisture content measured at 60 sampling occasions (whole data set) and predicted by SAHEL, (2) ^{14}C transferred into microbial biomass, measured at 60 sampling occasions (whole data set minus six eliminated outliers) and predicted by MOMOS, and (3) total remaining ^{14}C, measured at 66 sampling occasions (whole data set) and predicted by MOMOS.

slope of predicted versus measured values (equation (10)) does not differ significantly from 1. No bias was detected in moisture predictions, but the residual variance cannot be neglected. From the value of R^2 (Figure 2), SAHEL predictions explain only 74% of the total variance of the whole data set. Figures 3– show more precisely the correspondence between predicted and measured moisture at each sampling occasion for the six sites. The more marked outliers of all predictions concerned two samples at A(780) (Figure 5), three at A(1800) (Figure 6), and one at A(3400) (Figure 7).

[34] The two low-altitude sites, A(65) and A(165), under rain forest and savanna climate, were the most contrasting in terms of rainfall, water holding capacities, and soil moisture. In the rain forest environment, soil moisture predictions oscillated between 20 and 38% v/v except for one short dry period of 2–3 months during the first year of incubation where soil moisture fell to 15%. In contrast, the savanna site was characterized by a 5 month dry season with occasional rainfall events followed by a 7 month rainy season; the soil moisture was measured and predicted at less than 3% v/v during the dry season (except short water saturations after rainfall events) and at 5–14% during the rainy season. In terms of soil moisture, the seasonal forest site A(780) was intermediary between the two low-altitude sites, storing between 12 and 22% water in rainy season and only about 5% during the short 2 month dry season observed during the first year of incubation. The soil moisture content of the cloud forest site A(1800) was the highest of the six sites, near saturation at 38% v/v water in the rainy season, and between 15 and 38% during the short dry seasons. Soil moisture of the paramo site A(3400) was near 36% v/v water during the 7 months of the rainy seasons and about 15% in the marked 5 month dry seasons, except few rainfall events giving soil water oscillations between 15 and 36%. The observed rainfall seasonality was the same at the high-paramo site A(3968), but with lower soil water storage. Soil water oscillated around 20% in the rainy seasons and around 10% in the dry seasons.

[35] The combined effect of temperature and moisture gave contrasted predictions of the $f(T)f(\theta)$ factor acting on all the rate constants of the MOMOS model (equation (1)). It oscillated between 0.6 and 1 at A(65) except during a dry event when it fell to 0.35 (Figure 3b). The oscillations were more extended at A(165), between 0.4 and 0.95 in rainy seasons, and between 0.1 and 1 during the dry seasons (Figure 4b). Then the combined response factor progressively approached zero as altitude increased because of the slowing effect of low temperatures. At A(780), $f(T)f(\theta)$ oscillated near the range 0.6–0.8 during the rainy season and decreased to 0.3 in the dry season (Figure 4b). At A(1800) the combined response function was near the range 0.35–0.45 during the rainy season and fell to 0.1–0.35 during the dry periods (Figure 5b). At A(3400), $f(T)f(\theta)$ was in the range 0.15–0.25 during the rainy season and 0.1–0.15 during the dry season (Figure 6b). At A(3968), it fell to about 0.15 during rainy seasons and to 0.05–0.1 during dry seasons (Figure 7b).

3.2. Transfer of ^{14}C Into Microbial Biomass

[36] From F tests (equation (9) and Table 2) and considering the whole data set, there is a significant statistical correspondence between the MB-^{14}C measured in the soil bags and the predictions of MOMOS coupled with SAHEL. The model response is linear (Figure 2), and no bias was detected in the predictions, explaining 72% of the variability of the MB-^{14}C data. The dispersion of the points around the predicted versus observed line was not greater for MB-^{14}C than for moisture contents. Thus, MOMOS predictions of MB-^{14}C were robust and not very sensitive to moisture fluctuations. However, the significant MB-^{14}C adjustment of Figure 2 was obtained only after elimination of six of the 66 data points which were out of the distribution: the first points of the incubation at the highest sites (53 days of incubation at A(3400) and 44 and 71 days at A(3968)) and three middle points at A(780) (121, 184, and 240 days of incubation). Table 2 and Figures 3c, 4c, and 6c show significant MB-^{14}C predictions for A(65) with 8/10 predicted values inside the confidence intervals of measured values, A(165) with 9/10 predicted values inside the confidence intervals, and A(1800) with 10/10 predicted values inside the

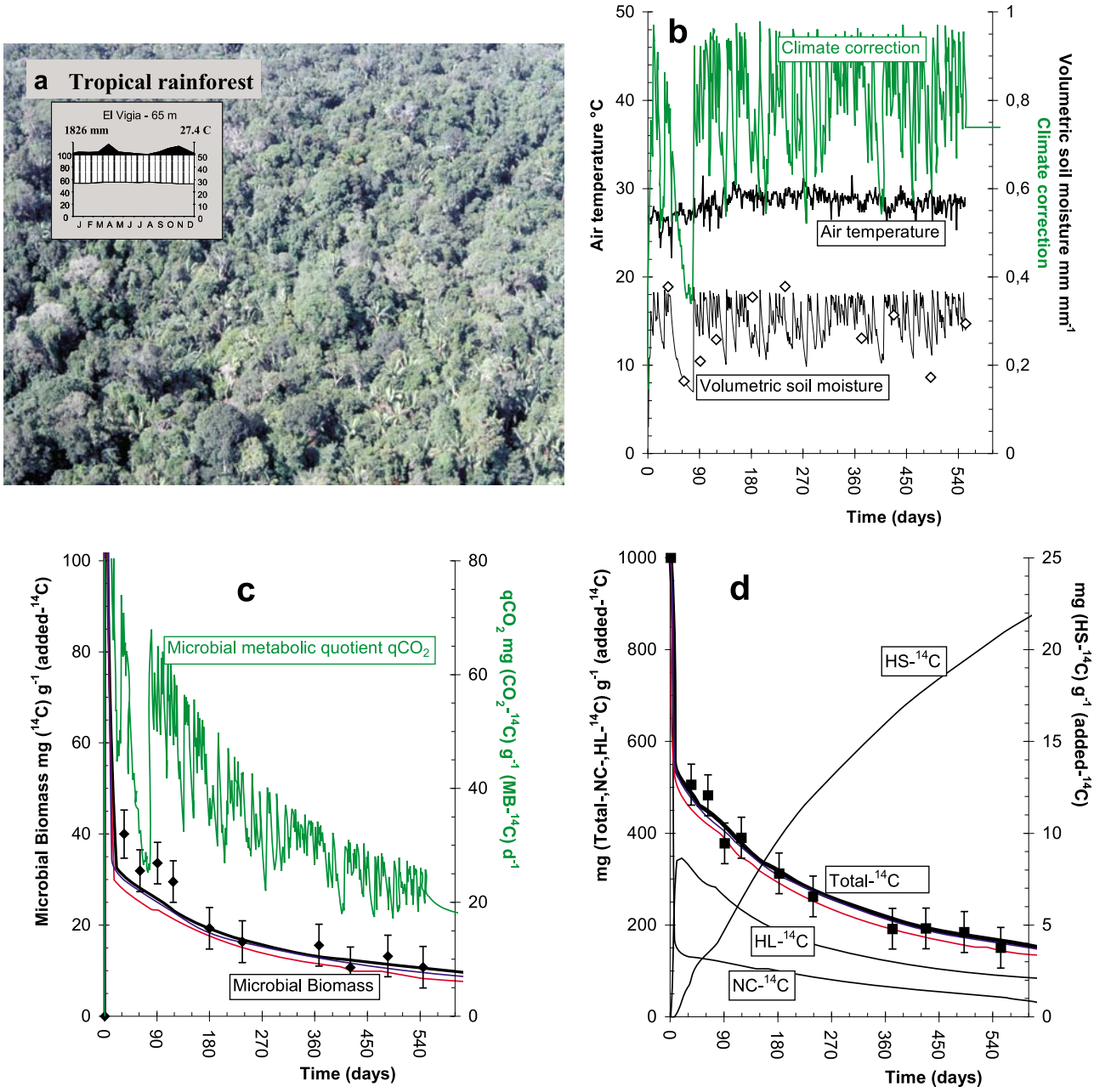

Figure 3. Dynamics of climate and organic transformations in soil of the tropical rain forest ecosystem A (65) of El Vigia: (a) natural typical vegetation and climate; (b) measured and modeled air temperature, volumetric soil moisture (diamonds, measured data four replicates; line, SAHEL prediction) and corresponding climate correction (green line) acting on the MOMOS model; (c) measured (points with 95% confidence intervals) and modeled (lines) microbial biomass and its metabolic quotient; black and green lines are predicted values using optimized respiration rate (k_{resp}), red line is predicted value using k_{resp} estimated by the pedotransfer function based on soil texture, and blue line is predicted value using k_{resp} estimated by the pedotransfer function based on soil pH; (d) measured (points with 95% confidence intervals) and modeled carbon mineralization (Total-^{14}C) and transfers from necromass compartments (NC-^{14}C) to labile (HL-^{14}C) and stable (HS-^{14}C) microbial metabolite compartments of the MOMOS model. See Figure 3c for meaning of line colors.

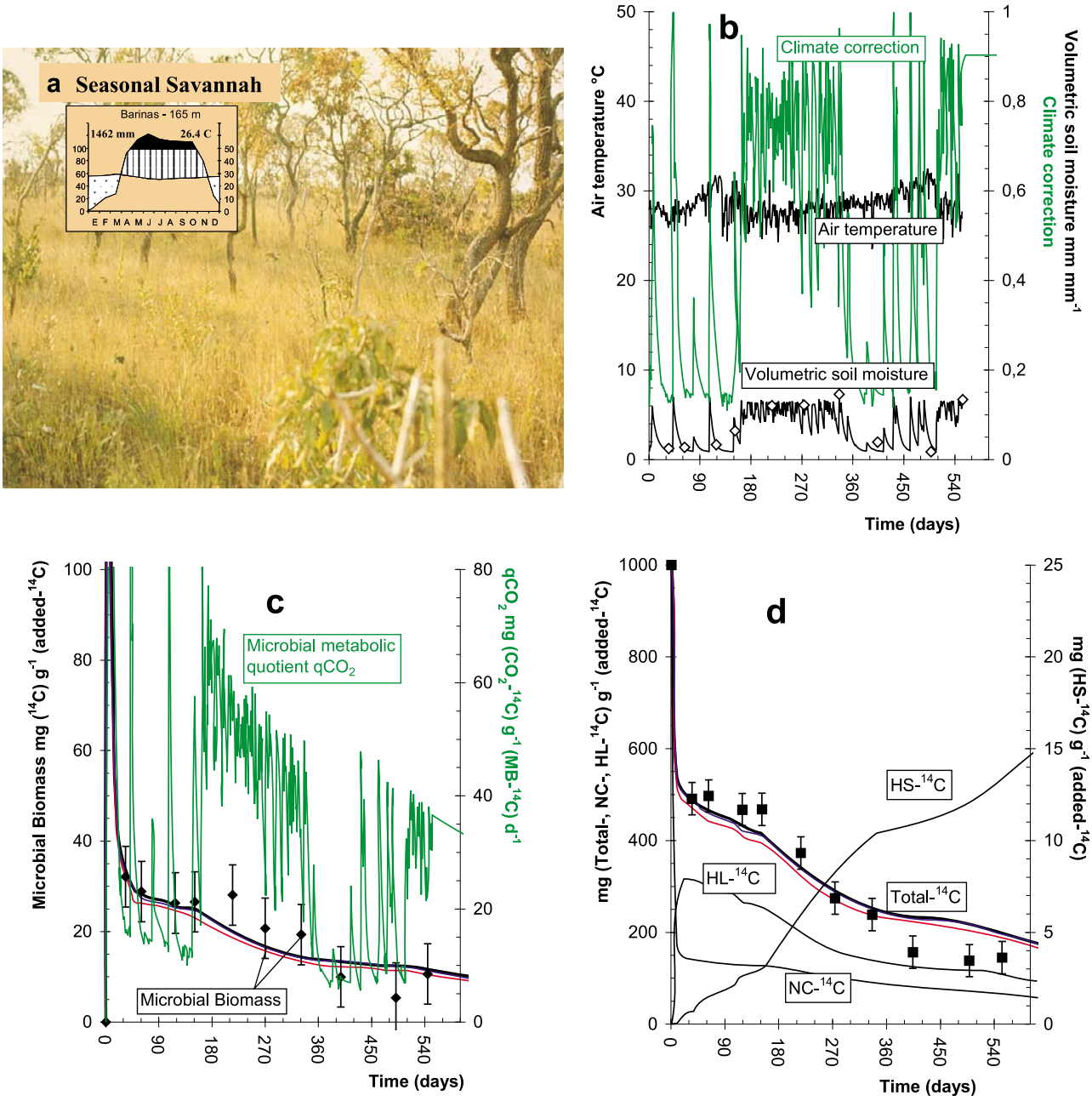

Figure 4. Dynamics of climate and organic transformations in soil of the tropical seasonal savannah A(145) of Barinas: see Figure 3 caption.

confidence intervals. For A(780) (Figure 5c), the seven first MB-^{14}C values, between 1 month and 1 year of incubation, were underpredicted by MOMOS; only the two last points were predicted inside the confidence intervals of measured values. In the two highest sites, A(3400) and A(3968) (Figures 7c and 8c), MOMOS overpredicted MB-^{14}C (predictions about 20% higher than the higher value of confidence interval of measured data). Only at 133 days of incubation for A(3400) and 123 and 183 days for A(3968) the predicted values were inside the confidence intervals of measured data.

[37] Despite the great differences in climatic conditions, the fraction of added ^{14}C which is measured and modeled as transferred from the added plant material to the microbial biomass was almost similar in each site. At A(65) (Figure 3c) it ranged from 40 at 1 month to 10 mg ^{14}C g^{-1} added-^{14}C at 18 months of incubation. At A(165) (Figure 4c) the range was 32 at 1 month to 5 mg ^{14}C g^{-1} added-^{14}C at 18 months of incubation. The level of ^{14}C transferred to MB increased slightly for mountain sites except A(1800). At A(780) (Figure 5c), the range was modeled at 40–15 mg ^{14}C g^{-1}

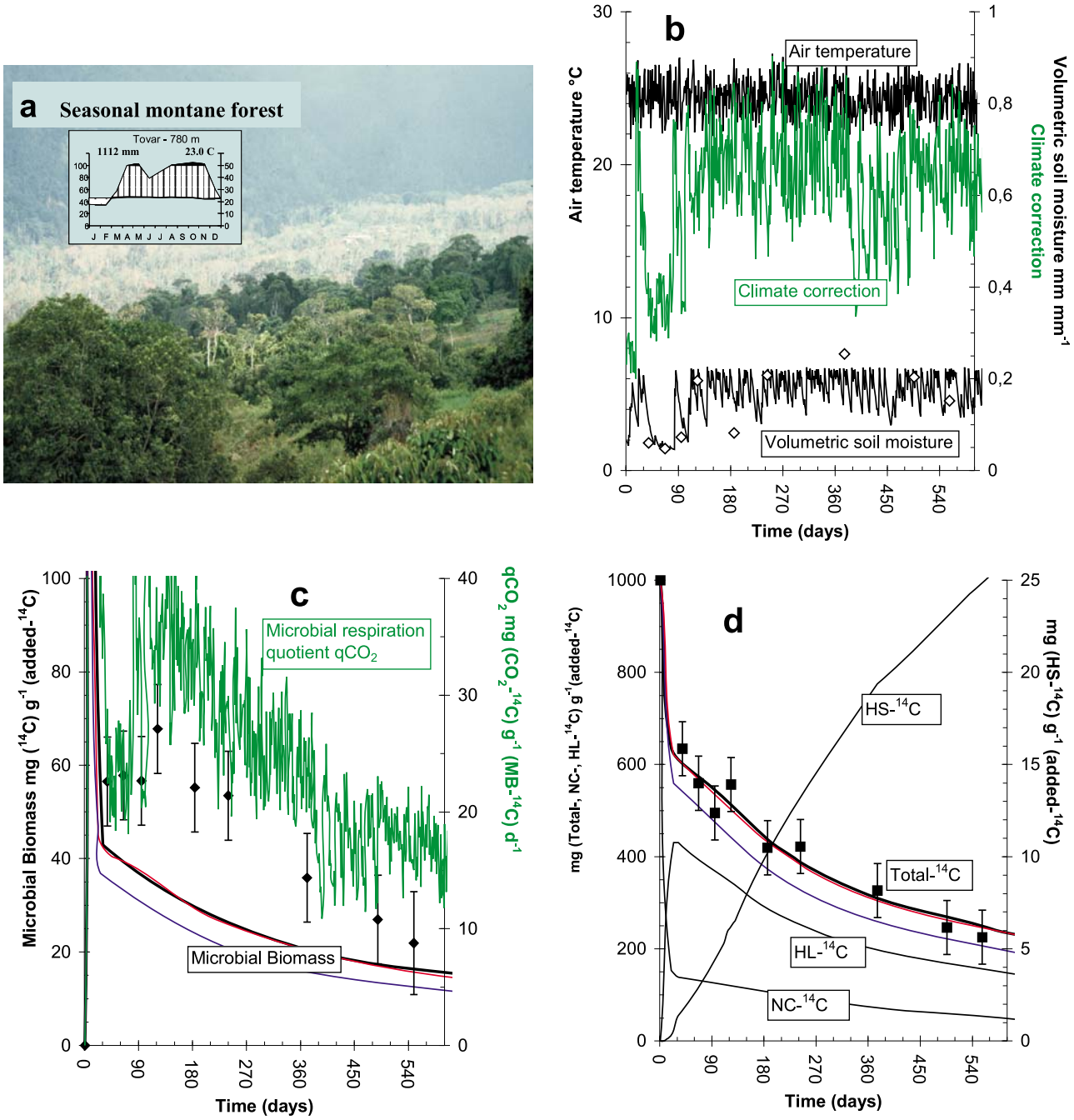

Figure 5. Dynamics of climate and organic transformations in soil of the mountain seasonal forest A(780) of Tovar: see Figure 3 caption.

added-^{14}C and measured at 65–20 mg ^{14}C g^{-1} added-^{14}C. At A(1800) (Figure 6c) it was measured and modeled at 40–12 mg ^{14}C g^{-1} added-^{14}C similarly to the A(65) site. At A(3400) (Figure 7c) and A(3968) (Figure 8c) the MB-^{14}C ranges were measured at 50–20 mg ^{14}C g^{-1} added-^{14}C and modeled at 50–30 mg ^{14}C g^{-1} added-^{14}C between 3 and 40 months of incubation. The effect of climate on the dynamics of MB-^{14}C appears to be most noticeable in the seasonal savanna site A(165) (Figure 4c) where the curve shape indicates (1) the fastest decrease of the initial peak in the first month of incubation (explained by the highest value of the respiration rate k_{resp}; see Table 2) and (2) a following stable period during the 5 month dry period, another slight decrease during the following 6 month rainy period, and another stabilization then another low decrease at the end. At A(65) (Figure 3c) and A(780) (Figure 5c) the climate effect on reduction of MB-^{14}C decrease was observed only during the first dry period between 1 and 3 months of incubation. The

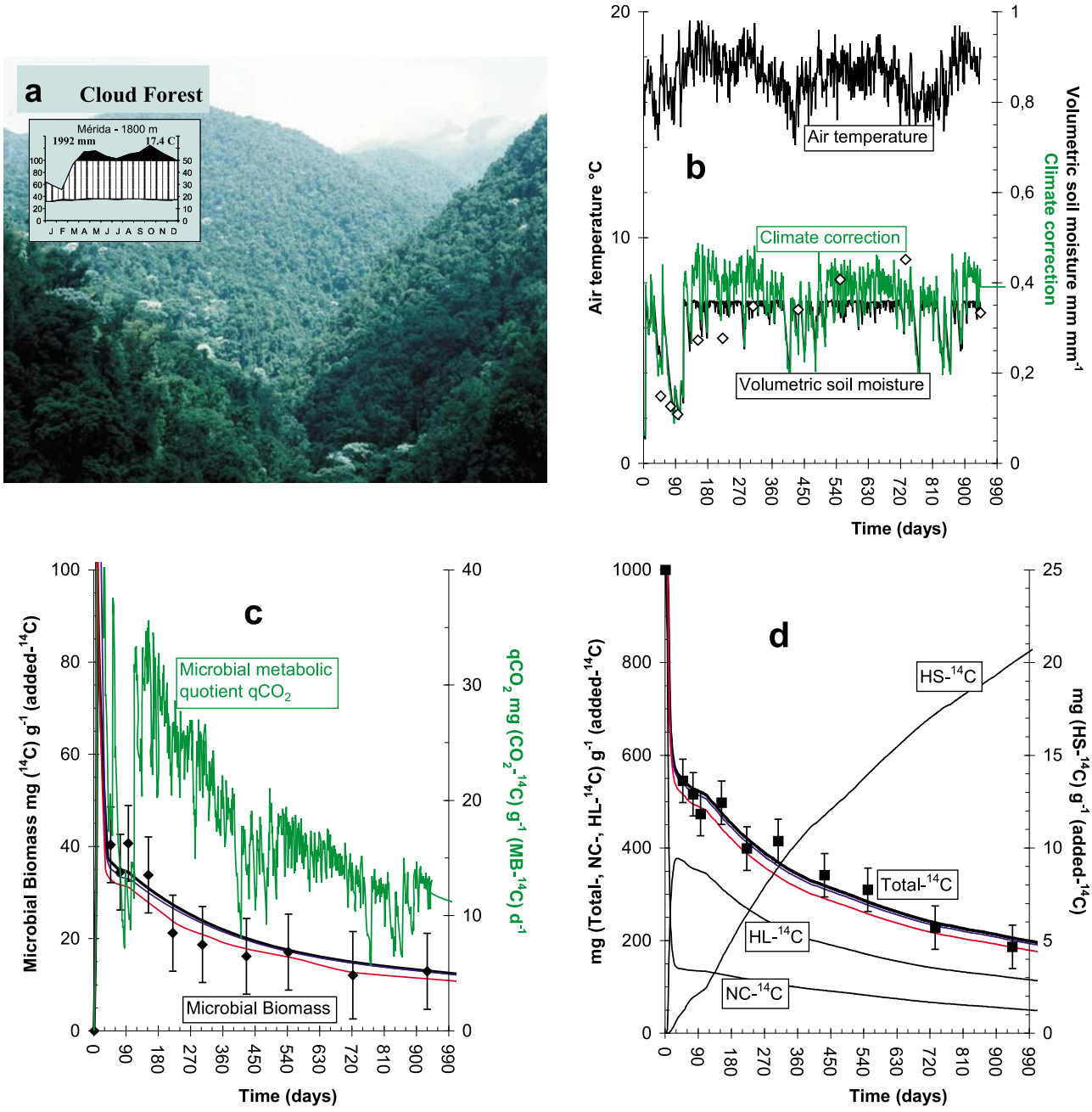

Figure 6. Dynamics of climate and organic transformations in soil of the cloud montane forest A(1800) of Mérida: see Figure 3 caption.

same was observed at A(1800) (Figure 6c) with additionally another slight slope change during the second dry period. The highest sites of A(3400) (Figure 7c) and A(3968) (Figure 8c) were characterized by (1) a higher time of decrease of the first initial MB-^{14}C peak since microbial respiration was lowered by climatic conditions and (2) slight changes of slope of MB-^{14}C curve with seasonal changes of rainfall.

[38] The effect of climate on the microbial metabolic quotient qCO_2-^{14}C (modeled only, not measured) was markedly higher than its effect on the level of MB-^{14}C. The metabolic quotient was the highest in the lower sites and decreased strongly with altitude and temperature (see section 4.2).

3.3. Total ^{14}C Remaining in the Soil and in the Humus Compartments

[39] *F* tests (equation (9)) of Table 2 show very significant MOMOS predictions of the total ^{14}C remaining in soil for the whole data set and for each site. The Figure 2 shows a linear response of total ^{14}C predictions, and no bias was detected (Table 2). MOMOS predictions explained 98% of the variability of the measured data with a residue distribution close

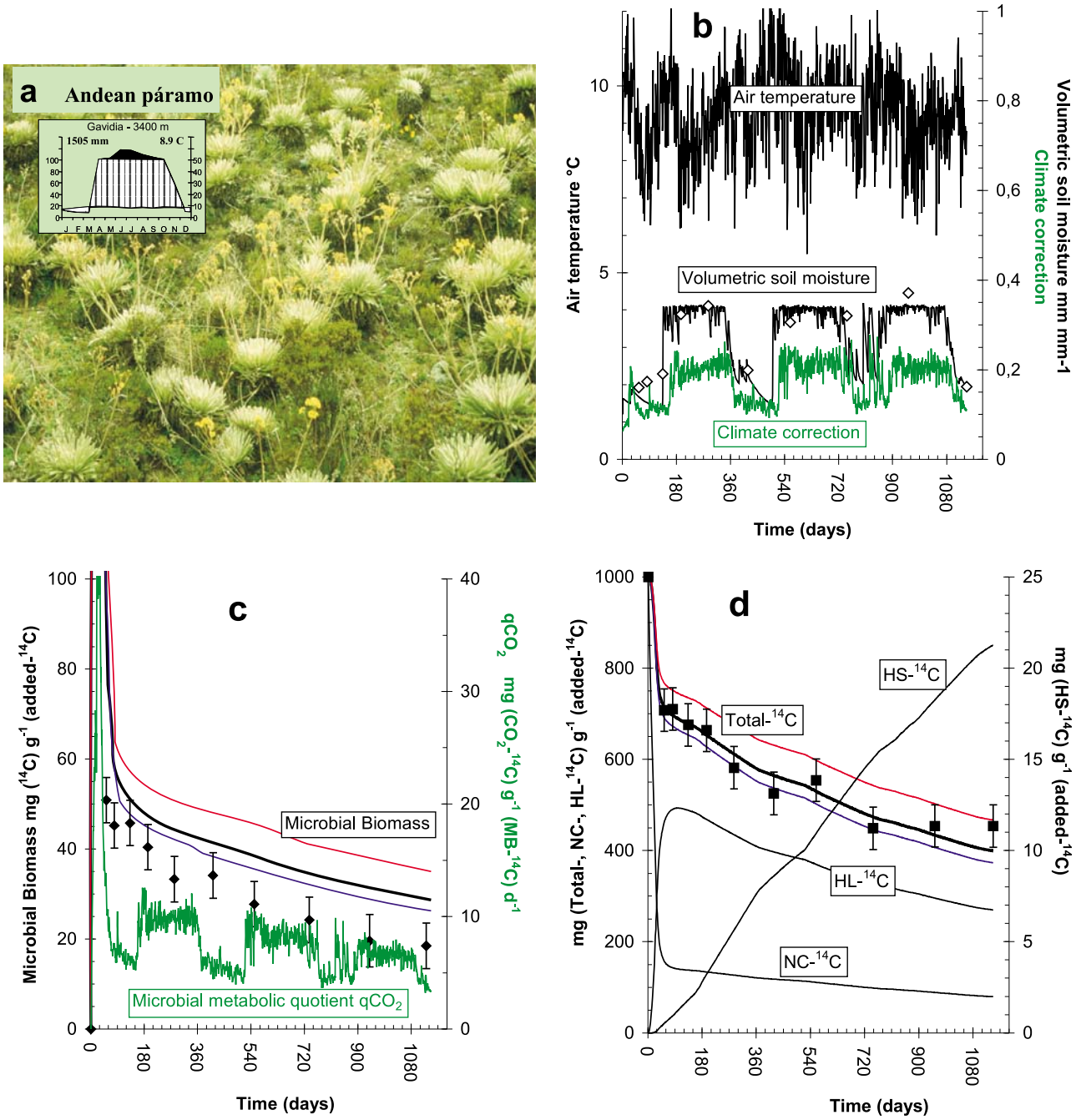

Figure 7. Dynamics of climate and organic transformations in soil of the Andean paramo A(3400) of Gavidia: see Figure 3 caption.

to the 1:1 line of predicted versus measured values. Total-^{14}C predictions were more precise than soil moisture or MB-^{14}C predictions (Figure 2), and MOMOS appears as a robust model of total C changes giving predictions not very sensitive to changes in moisture or microbial contents.

[40] The remaining ^{14}C increased with altitude, giving three types of decay curves. In the low-altitude sites A(65) and A(165), about 50% of the ^{14}C was lost in the first week of the experiment, then total-^{14}C decreased more slowly to about 20% of the added ^{14}C at 20 months of incubation. At the mean altitudinal sites A(780) and A(1800) about 40% of added-^{14}C was lost during the first month to 75–80% at 20 months of incubation. At the highest sites of A(3400) and A(3968), about 30% of added-^{14}C was respired during the first month and 55% at 38 months of incubation. The shape of the total-^{14}C prediction curves was similar to that of MB-^{14}C curves (see section 3.2), showing decreases of slope in dry periods and increases in rainy periods.

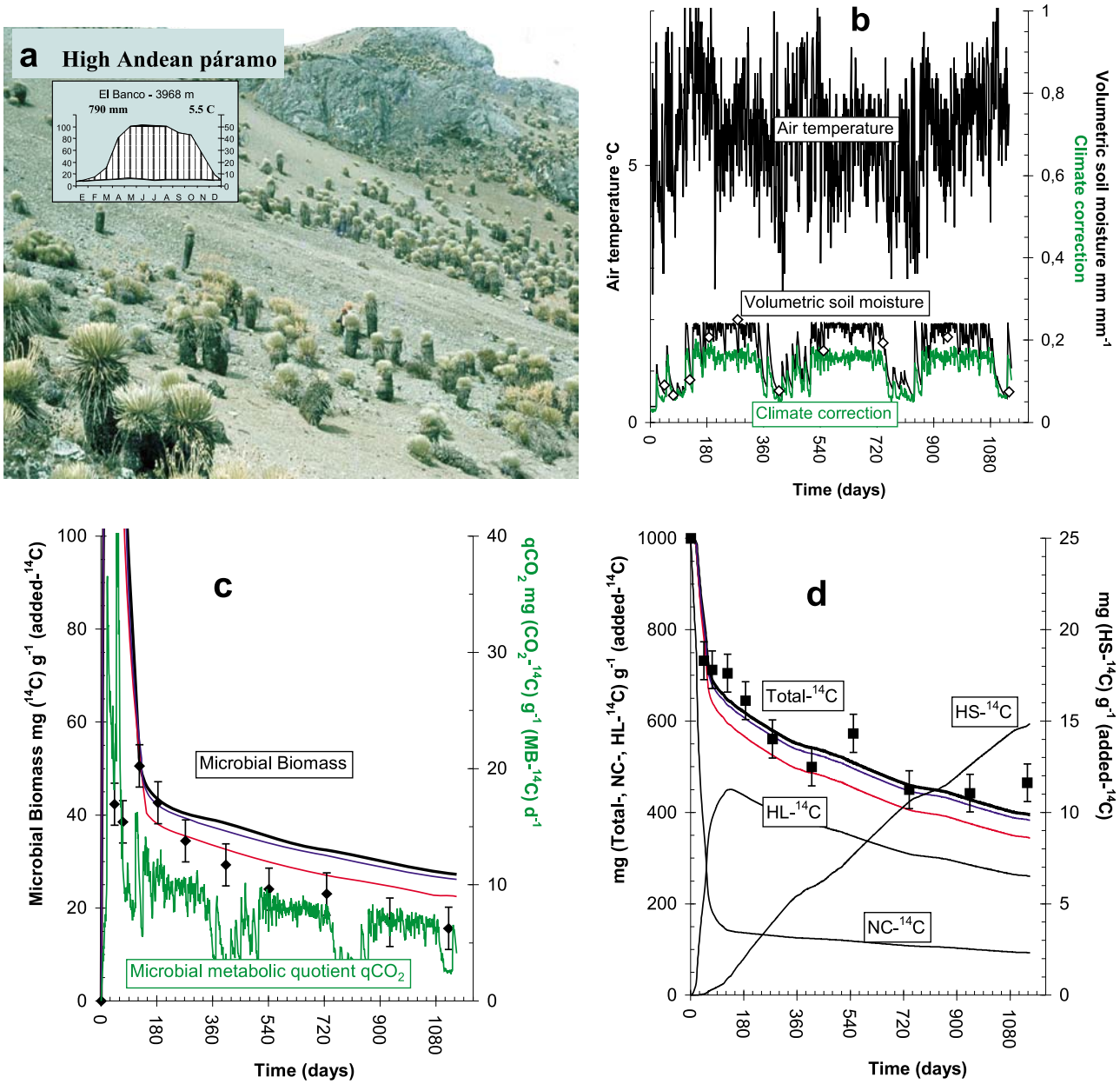

Figure 8. Dynamics of climate and organic transformations in soil of the high Andean paramo A(3968) of El Banco: see Figure 3 caption.

[41] In all sites, MOMOS simulates a quick exhaustion of the labile compartment VL of the added ^{14}C-straw. The time necessary to complete VL decomposition was found dependent on moisture conditions: 13 days at A(65) against 27 days at A(165). This decay time was also a function of temperature, increasing with altitude: 23 days at A(780), 30 days at A(1800), 78 days at A(3400), and 120 days at A(3968). After the VL exhaustion, ^{14}C-VS was modeled at a lower decrease controlled again by climatic conditions. At 600 days incubation time the remaining ^{14}C in stable necromass was modeled at 37, 60, 48, 77, 108, and 115 mg NC-^{14}C g^{-1} (added-^{14}C) at A(65), A(165), A(780), A(1800), A(3400), and A(3968), respectively. The rapid initial VL assimilation induced the pronounced MB-^{14}C peak simulated at the beginning of incubation and a high ^{14}C transfer to the humus labile compartment (HL) composed by microbial metabolites. When VL was completely decomposed (see above), the modeled fraction of added-^{14}C that was found in the HL-^{14}C was 30–35% at the two lower sites, A(65) and A(165), 40–45% at the mountain sites, A(780) and A(1800), and 45–50% at the highest sites, A(3400) and A(3968). Afterward, the HL-^{14}C represented the new main energy source for microorganisms, and its curve shape of decrease was modeled as similar to that of total-^{14}C. A small part of HL was

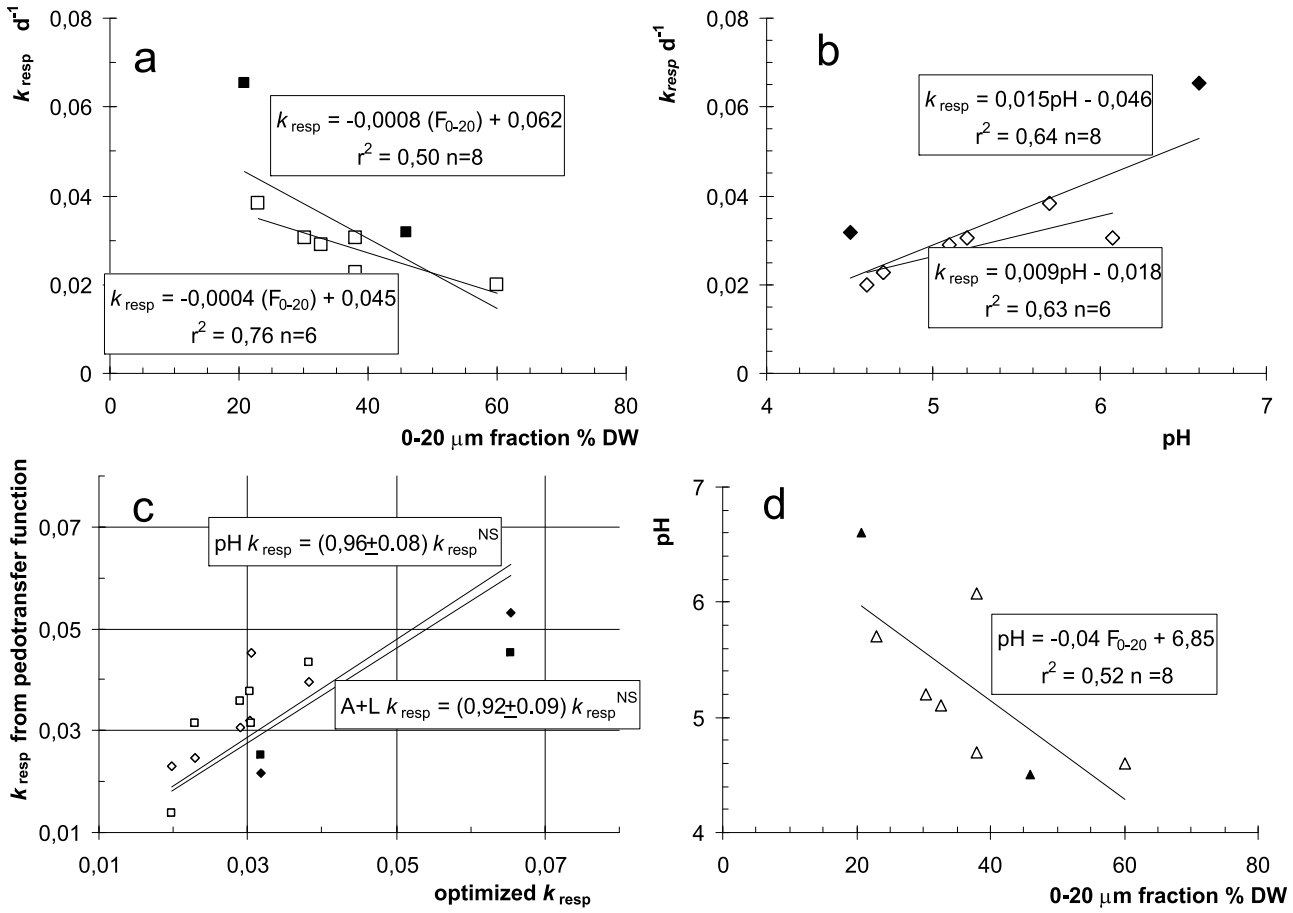

Figure 9. Proposition of soil transfer functions (PTF) linking the microbial respiration rate k_{resp} to soil texture and/or soil pH; the two plain black points come from the calibration sites, and six other open points come from the validation sites: (a) PTF between k_{resp} to 0–20 μm soil fraction (F_{0-20}); (b) PTF between k_{resp} and soil pH; (c) validity of k_{resp} predictions by PTFs; and (d) link between pH and F_{0-20} in the studied Andean sites.

also modeled as sequestered in the stable HS compartment, representing at 600 days of incubation 29, 38, 34, 29, 21, and 22 mg HS-^{14}C g^{-1} (added-^{14}C) in order of lowest to highest altitude.

3.4. Relationships Between Respiration Rate and Soil Properties

[42] With the same quality of labeled straw in the two sites of the calibration experiment as in the six sites of the validation experiment, MOMOS enabled us to predict total-^{14}C as well as MB-^{14}C evolution using unchanged values of six of its seven parameters (see section 2.3) and optimizing only the value of the microbial respiration rate k_{resp} in each site. This is a demonstration of the important link between microbial respiration and soil properties. The goal was then to explore the possible relationships within k_{resp} and different soil properties in the altitudinal transect. The soil properties available at the moment in each site are summarized in Table 1: C and N content, textural characteristics, soil pH, cation exchange capacity, water holding capacity, and water content at wilting point. The last water storage properties were already used in MOMOS predictions by the intermediary of the SAHEL model. The only other possible relationships with microbial respiration found from this data (not significant at 5% level) were (1) a negative linear relationships between k_{resp} and fine 0–20 μm fractions (Figure 9a) of the soils (clay + silt fraction), expressing that microbial respiration was lowered by fine textures; and (2) a positive linear relationships between k_{resp} and soil pH in water (Figure 9b), expressing that microbial respiration was lowered by soil acidity. These two kinds of relationships occurred possibly because pH and the 0–20 μm textural fraction are related in these acidic tropical materials (not significant at 5%; see Figure 9d). The two black square points of Figure 9 come from the previous calibration experiment of MOMOS (another plot from the Venezuelan paramo and a plot from the Bolivian puna), and the open square points come from the validation experiment of this paper. So Figure 9 showed differences between the two experiments and relationships found for the whole data set (calibration + validation, n = 8) or for the validation set only (n = 6). The quality of the two adjustments k_{resp} versus pH (Figure 9b) was equivalent, expressing 63–64% of the k_{resp} variability, but

k_{resp} was better adjusted to the fine fraction when only the validation data set was used (Figure 9a). To extend the model to a larger geographic zone for global change predictions, the most robust pedotransfer functions must be chosen. We propose to retain the relationships calculated using the two calibration and validation experiments, even if they are found less significant. Figure 9c shows predicted versus optimized k_{resp} values for the whole data set; no bias was detected in prediction of k_{resp} versus pH or k_{resp} versus 0–20 μm fraction.

[43] The pedotransfer functions showed in Figures 9a and 9b (with $n = 8$) were then used to calculate new MOMOS predictions replacing optimized k_{resp} values (black curves in Figures 3–8) by k_{resp} values calculated from rates of 0–20 μm soil fraction (red curves in Figures 3–8) or soil pH in water (blue curves) in each site. Most of total- and MB-^{14}C predictions remain highly significant when one or the other pedotransfer functions were used. At A(65), A(165), A(1800), and A(3968) (Figures 3, 4, 6, and 8), the predictions using k_{resp} calculated from soil pH were almost the same as those using the optimized k_{resp}. At A(780) (Figure 6), the predictions using optimized k_{resp} or k_{resp} calculated from $F_{0–20}$ were the same. At A(65) (Figure 3), A(165) (Figure 4), and A(1800) (Figure 6), they were equivalent. At A(780), the predictions using k_{resp} calculated from soil pH increase slightly the underestimation of MB-^{14}C and underestimate three points of the total-^{14}C, the other predictions remaining inside the confidence intervals of measured data. At A(3400), the prediction using the $F_{0–20}$ fraction increases slightly the overestimation of MB-^{14}C and overestimates four points of total-^{14}C. Inversely, at A(3968), the $F_{0–20}$ pedotransfer function improves the prediction of the MB-^{14}C but underestimates three points of total-^{14}C. In each site the error in the prediction MB- or total-^{14}C using pH or $F_{0–20}$ pedotransfer functions was less than 10%.

4. Discussion

4.1. Relevance of MOMOS Compared to Apparently More Simple Models

[44] MOMOS allowed us to adequately predict total and microbial ^{14}C dynamics during the decomposition of a standard plant material (wheat straw) in six extremely contrasting tropical environments using only one parameter specific to each site (k_{resp}) instead of the two or three site specific parameters necessary in previous analysis using the same database to predict only total ^{14}C by two exponential models [*Coûteaux et al.*, 2002; *Braakhekke and de Bruijn*, 2007]. Furthermore, only this parameter k_{resp} is related to soil properties. This study demonstrates that climate, together with basic soil properties such as texture and pH, is the main driver of soil organic matter dynamics when a large range of conditions are considered (98% of the total ^{14}C variability was explained). Other specific soil characteristics, such as the composition of soil microbial communities, seem to be of secondary importance. MOMOS allowed a much better description and understanding of soil organic matter dynamics than the sole statistical analysis of this data previously performed, showing more clearly the strong connection of decomposition to climate.

[45] The following discussion will be centered in the three aspects more relevant to the description of the soil organic matter dynamics under different environments: the choice of the climate response functions (section 4.2) and the microbial activity as the main driver of carbon transformations and how respiration is influenced by climate (section 4.3) and soil properties (section 4.4).

4.2. Temperature and Soil Moisture Response Functions

[46] The temperature response functions applied to describe the dynamics of organic matter decay come from the laws of chemical kinetics, generally Arrhenius or Van't Hoff laws, acting on rate constants of compartment models as described by many authors like *Rodrigo et al.* [1997], *Kätterer et al.* [1998], *Lomander et al.* [1998], *Leirós et al.* [1999], or *Rey et al.* [2005]. Literature data on models previous to MOMOS described other common parameters, such as flow partitioning (efficiency factors), not considered to be related to temperature or moisture. The Arrhenius law, $f(T)$, of equation (1) could be written:

$$f(\mathrm{T}) = e^{-E/RT}$$

where E is the activation energy, R the constant of perfect gases, and T is the absolute temperature. The Van't Off expression (equation (2)) was based on the ratio of the law at two temperatures and does not need the use of the E/R ratio, Q_{10} being the rate increase for a temperature increase of 10°C. Other response functions are available from literature, like quadratic corrections, but Q_{10} has probably been the most used and was chosen for this work. Our attempts to optimize simultaneously Q_{10} and T_{opt} values (equation (2)) gave undetermined multiple solutions. Different attempts to fix values of T_{opt} were tried; finally, the value of 28°C, just above the mean temperature of the warmer sites, was chosen for all situations, although the hypothesis of optimal temperature conditions not depending on mean annual temperature is questionable. On the same data, the previous studies of *Coûteaux et al.* [2002] and *Braakhekke and de Bruijn* [2007] used T_{opt} of 25°C and 27°C, respectively, for all sites. After fixing T_{opt}, the Q_{10} value was optimized for each site, but no significant relationship between the optimized Q_{10} values and mean temperatures or other variable was detected, although some authors suggested decreasing Q_{10} values with temperature [e.g., *Dalias et al.*, 2001]. Finally, we chose to retain the mean of the obtained values, giving $Q_{10} = 2.2$ for all sites, which was the value already used by *Coûteaux et al.* [2002] for the same experiment and by *Coûteaux et al.* [2001] for a ^{13}C experiment in an European latitudinal transect. The value of 3.75 proposed for Q_{10} by *Braakhekke and de Bruijn* [2007] seems high compared to most of literature data.

[47] There is not a unified relationship to link soil moisture content and C evolution in decomposition models. Sometimes, relationships were not given as formulae but with graphs showing moisture correction factors ($f(\theta)$ of equation (3)) varying between 0 and 1. Some models need not soil physical data but approximate $f(\theta)$ to water balance at the level of climate and ecosystem. For example, *Parton et al.* [1987] proposed a graphical link between $f(\theta)$ and the monthly ratio

$\frac{\text{precipitation PPT}}{\text{potential evapotranspiration PET}}$ where $f(\theta)$ increased from 0.25 to 1 when PPT/PET increased from 0 to 1.25. *Jenkinson* [1990] proposed a comparable graphical response function linking $f(\theta)$ to topsoil moisture deficit TMD calculated from the balance between mean monthly evapotranspiration and rainfall, giving $f(\theta) = 1$ for TMD between 0 and 20 mm water, then $f(\theta)$ decreasing linearly from 1 to 0.2 when TMD increased from 20 to 50 mm. Other more precise relationships consider the soil material for its capacity to store water. For *van der Linden et al.* [1987], $f(\theta)$ was given at 1 for soil capillary suction pF between 1 and 2.5, then $f(\theta)$ decreased linearly from 1 to 0 when pF increased from 2.5 to 5. For *Hansen et al.* [1991] and *Mueller et al.* [1997], $f(\theta)$ decreased also linearly from 1 to 0 when pF increased from 2 to 5. Other authors like *Andrén and Paustian* [1987] proposed to link the response function to water potential Ψ in Mpa by the relation:

$$f(\theta) = \log(\Psi_{min}/\Psi)/\log(\Psi_{min}/\Psi_{max})$$

where Ψ_{min} and Ψ_{max} were boundary values for minimum and maximum water potentials.

[48] *Lomander et al.* [1998] proposed a quadratic moisture function:

$$f(\theta) = 1 - d_1(\theta^2_{max} - \theta^2)$$

where θ^2_{max} was the highest water content in the soil and d_1 was a constant.

[49] *Leirós et al.* [1999] and *Wang et al.* [2004] proposed linear corrections with moisture expressed as its ratio to water holding capacity:

$$f(\theta) = a + b\ \theta/\text{WHC}$$

[50] In the same way, *Rey et al.* [2005] added a squared polynomial term giving a parabolic correction with relative soil moisture, which possibly smoothed the values of correction factor near the boundary limits. Previously, *Rodrigo et al.* [1997] detailed possible formulae for soil moisture correction and emphasized that N mineralization rates could be related to relative soil water content or to the log of soil water potential, the two types of formulation being considered as equivalent at least for $f(\theta)$ response functions. Moreover, they indicated from some studies that the constants a and b of the relation $f(\theta) = a + b\ \theta/\text{WHC}$ were generally found near 0 and 1, respectively, which gave equation (3) used in this paper. *Antonopoulos* [1999] proposed also this relationship among more sophisticated possible equations. Though equation (3) appeared as a simplification implying a sudden change of the slope of $f(\theta)$ at boundary values and did not indicate a $f(\theta)$ reduction for waterlogged soils (the experimental sites of this study were well-drained and not waterlogged during significant periods), other equation choice did not improve the accuracy of MOMOS predictions in these systems. Possibly, differences in formulations of $f(\theta)$ equation were compensated for by slightly different optimized values for the respiration rate parameter (see section 2.3).

[51] The coupling of MOMOS with SAHEL was satisfactory for this validation experiment, but other more precise water models have to be used in soils with saturated water flux. SAHEL explained 74% of the variability of the whole data set; the available weather, soil physics, and plant cover data cannot enable more reliable results. SAHEL needs the dynamics of the leaf area index to split evapotranspiration between its two components and the distribution of roots in the soil profile to perform the partitioning of transpiration between the layers. For some sites the required estimations and corrections of climate data probably contributed to increase the discrepancies between measured and predicted soil moisture. However, despite the possible limitations of SAHEL predictions, the precision was enough to obtain a good description of the daily soil water dynamics and its effect on decomposition.

4.3. Microbial Respiration and Climate Conditions

[52] This data and modeling exercise showed that ^{14}C mineralization and transfers were controlled by microbial respiration almost independently of the level of ^{14}C remaining into microbial biomass. At the incubation end, MB-^{14}C was measured between 10 and 20 mg MB-^{14}C g^{-1} added-^{14}C in all sites (see details in section 3.2), when qCO_2-^{14}C were predicted very different in each site. In the rain forest climate of A(65), qCO_2 was predicted between 20 and 80 mg CO_2-^{14}C g^{-1} MB-^{14}C d^{-1} during the first 3 months and between 20 and 25 at the end of incubation (Figure 3c). The mean qCO_2 levels were similar in the savanna climate of A(165) with a more extended oscillating range between 10 and 80 mg CO_2-^{14}C g^{-1} MB-^{14}C d^{-1} during the first 3 months and between 5 and 40 mg CO_2-^{14}C g^{-1} MB-^{14}C d^{-1} at the end of incubation (Figure 4c), in accordance with larger oscillations of the $f(T)f(\theta)$ climatic factor (equation (1) and Figure 3b). Then qCO_2 decreased with increase of altitude and corresponding decrease of temperature and $f(T)f(\theta)$ values. At A(780) it oscillated between 20 and 40 mg CO_2-^{14}C g^{-1} MB-^{14}C d^{-1} during the first 3 months and between 12 and 23 at the end of incubation (Figure 5c). At A (1800) the oscillating range decreased to 5–35 mg CO_2-^{14}C g^{-1} MB-^{14}C d^{-1} during the first 3 months and to 5–15 at the end of incubation (Figure 6c). At A(3400) a first peak of 40 mg CO_2-^{14}C g^{-1} MB-^{14}C d^{-1} was reached only during the early weeks of incubation, and other qCO_2 values oscillated in the range 5–12 mg CO_2-^{14}C g^{-1} MB-^{14}C d^{-1} (Figure 7c). The respiration was again reduced in the highest altitude site A(3968), the first peak being limited to about 35 mg CO_2-^{14}C g^{-1} MB-^{14}C d^{-1}, the other values oscillating in the range 2–9 mg CO_2-^{14}C g^{-1} MB-^{14}C d^{-1} (Figure 7c) with $f(T)f(\theta)$ values already less than 0.2 (Figure 8b).

[53] The predicted qCO_2 values for the low-altitude sites were in the range of those found by *Anderson and Domsch* [1993] in different temperate forest soils measured at 22°C on samples collected in early spring: lowest values at about 20 mg CO_2-C g^{-1} (MB-C) d^{-1}, highest values at about 75 near our predicted initial peak. L. Sarmiento (unpublished Ph.D. thesis, 1995) found in the same area of the Venezuelan Paramo, under field conditions, qCO_2 values between 10 and 48 mg CO_2-C g^{-1} (MB-C) d^{-1}, with the highest values obtained after the incorporation of a green manure. This was comparable to $q^{14}CO_2$ values predicted during the rainy season in the site A(3400) of this experiment. For another paramo soil, *Sarmiento and Bottner* [2002] measured in an

experiment where ^{14}C labeled straw was incubated in laboratory optimal conditions (26°C and 80% of field capacity) a $q^{14}CO_2$ of 113 after 33 days and 26 g CO_2-^{14}C g^{-1} MB-^{14}C d^{-1} after 80 days which was near the range of the plain sites predicted from this experiment and higher than our predicted paramo values. This suggests that the level of C sequestration in the mountain sites could be highly reduced by increase of global temperature, which could increase again the greenhouse gas effect.

4.4. Microbial Respiration and Soil Properties

[54] Positive relationships between the C content of soils and those of their fine fractions were often reported [e.g., *Feller and Beare*, 1997]. Numerous labeling experiments showed also that fine soil texture generally reduce ^{14}C mineralization [e.g., *Sørensen*, 1981; *Bo and Xin-Xiong*, 1993; *Ladd et al.*, 1992; *Saggar et al.*, 1996, 1999]. In accordance with our results, a protecting effect has been noted also for MB-^{14}C and attributed to clays [*van Veen et al.*, 1985; *Ladd et al.*, 1995] or allophanic materials [*Saggar et al.*, 1994]. *Martin and Haider* [1986] ascribed the effect of clays (and especially allophanic clays) to the stabilization of carbon in humus. From *Thomsen et al.* [1999], texture effects were indirect: soil structure controls the soil pore system which defines water limitations for the decomposer organisms. From *Schjønning et al.* [1999], O_2 diffusion becomes more limiting for microbial activity when water-filled pore volume increases and air-filled pore volume decreases, with critical levels of air diffusivity for aerobic biochemical processes at an air-filled pore volume less than 20–30% of the total pore volume. From the ratios of soil moisture contents/WHC of our experiments (Figures 3b to 8b), these critical levels were exceeded at most incubation times for five of the six sites, except during dry periods which were especially marked at the savanna site. This could explain the soil C content measured in the high range of 37–101 g C kg^{-1} (soil) in the five more humid sites and only at 14 g C kg^{-1} (soil) at the driest site A(165) (Table 1).

[55] Fine texture has not already been identified as the main factor of C sequestration. In New Zealand soils, the correlation of C with clays was not observed by *Percival et al.* [2000] who noted a correlation between C and Al extracted by a pyrophosphate solution. *Poulenard et al.* [2003] explained the unusually fine porosity and the related hydraulic properties of humic soils of the Ecuadorian paramo (volcanic origin) by a large amount of organo-mineral colloids even in absence of allophanic materials. In the high Andean mountains under acid rock-material conditions, the presence of free aluminum hydroxides and exchangeable Al in the soils could limit the biological activity. At Gavidia (A(3400)), *Abadín et al.* [2002] found a free alumina content of 25 g kg^{-1} soil which easily exceeds the threshold of 10 g kg^{-1} soil for which *Gonzalez-Prieto et al.* [1996] found a significant decrease of mineralization rate.

[56] Most of the available decomposition models propose adjustment factors relating only the texture effect on decomposition processes [*van Veen et al.*, 1985; *Parton et al.*, 1987; *Hansen et al.*, 1991; *Bosatta and Agren*, 1997; *Hassink and Whitmore*, 1997]. The two proposed relationships of this work (Figure 9) enabled us to link microbial respiration to either (1) rates of 0–20 μm textural fraction or (2) soil pH. Figures 3–8 show the robustness of these relationships for total- and MB-^{14}C predictions in the six studied sites. Consequently, we propose to extend their use as pedotransfer functions for carbon predictions in all situations where data on soil texture or/and soil pH (especially in acidic media) are available.

5. Conclusion

[57] This experimental study using ^{14}C tracer in six highly contrasted sites enabled us to validate the hypotheses of the previous MOMOS calibration carried out in two high-altitude tropical sites:

[58] 1. The MOMOS schemes centered on the functioning role of microbial biomass, first established in two high mountain ecosystems, can be transposed to other very contrasted and extended tropical environments as well as to other mountain ecosystems,

[59] 2. For the same quality of the organic input in all experimental sites, the values of six of the seven optimal rate parameters of MOMOS can remain unchanged and similar to the initial calibration values; for a given input, microbial growth and humification beginning by microbial mortality in the different sites are driven mainly by functions of temperature and soil moisture conditions.

[60] 3. The proposed temperature response function was the exponential law using a Q_{10} of 2.2 and an optimal temperature of 28°C, and the proposed equation for moisture response was the ratio of daily soil moisture (modeled by SAHEL) to water holding capacity,

[61] 4. The only parameter that was found to be related to both climate conditions and soil properties was the rate of microbial respiration driving the C mineralization.

[62] So this experiment enables us to propose MOMOS as an accurate tool to predict both C humification in soils and CO_2 exchanges with atmosphere. The simultaneous evolution of five compartments was modeled using only six optimal parameter values (for optimal conditions of temperature and moisture) found invariable for all sites and one site-dependent parameter: the optimal respiration rate. Finally, MOMOS appears as the best tool to reduce complexity. Only 12 parameter values (six site-dependent values plus six constant values) linked to climate response functions were necessary to predict both microbial mineralization and humification. In contrast, the previous attempts to predict only mineralization with two-compartment models needed 18 parameter values for all sites in the first version and 13 parameter values in the second version. To spatialize the use of MOMOS, two soil transfer functions are proposed, bounding microbial respiration to (1) soil texture or (2) soil pH. The proposed linear regressions come from eight much contrasted sites (two for calibration and six for validation experiment). Despite that their adjustments were found not significant at 5% risk, the soil transfer functions enabled us to predict significantly the evolution of both total- and microbial-^{14}C measurements of each site. This paper shows the robustness of the model, which predicted ^{14}C data linearly adjusted to measurements with better repeatability than that of soil moisture (predicted by SAHEL) and respiration coefficient (predicted by soil texture or pH data) in soil.

[63] Both calibration and validation experiments enabled us to understand the mechanisms binding microbial respiration to C cycle. Low temperature reduces microbial respiration as well as other processes of microbial mortality and growth, which tend to increase C sequestration when altitude increases. Dry conditions can strongly reduce and stop all the decomposition processes. But the temperature and moisture reductive effects can be compensated for by a better microbial respiration if oxygen access is not lowered by too fine texture and microbial activity is not reduced by aluminum complexes in acid conditions. It was the case of two sites: one at low altitude (Barinas, A(165), validation experiment) and another one in the high mountain environment (Bolivian puna, calibration experiment) where a very low C sequestration was measured and modeled, despite climate conditions less favorable to mineralization than in the other sites. This modeling data shows that decomposition processes are not primarily controlled by the level of microbial populations but by their respiration quotient: climate conditions and soil physical constraint acting on microbial respiration are the main factor which regulate the C cycle.

[64] **Acknowledgments.** This study was framed within the bilateral France-Venezuela cooperation program ECOS-NORD V07A01 (Modeling soil organic mater in Venezuelan ecosystems and its application to fertility management and carbon sequestration) and partiality financed by CDCHT-ULA (project C-765-95-01-B) and FONACIT (F-2002000424). We would like to thank Zulay Mendez for her technical assistance in the laboratory and Yann Martineau (SETEC International, F-13127 Vitrolles, France) and Klaas Metselaar (Soil Physics, Wageningen University, Netherlands) for the orientation in the modeling process.

References

Abadín, J., S. J. González-Prieto, M. C. Villar, and T. Carballas (2002), Successional dynamics of soil characteristics in a long fallow agricultural system of the high tropical Andes, *Soil Biol. Biochem.*, *34*, 1739–1748, doi:10.1016/S0038-0717(02)00161-X.

Adair, E. C., W. J. Parton, S. J. Del Grosso, W. L. Silver, M. E. Harmon, S. A. Hall, I. C. Burke, and S. C. Hart (2008), Simple three-pool model accurately describes patterns of long-term litter decomposition in diverse climates, *Global Change Biol.*, *14*, 2636–2660.

Anderson, T. H., and K. H. Domsch (1993), The metabolic quotient for CO_2 (q_{CO2}) as a specific activity parameter to assess the effect of environmental conditions such as pH on the microbial biomass of forests soil, *Soil Biol. Biochem.*, *25*, 393–395, doi:10.1016/0038-0717(93)90140-7.

Andrén, O., and K. Paustian (1987), Barley straw decomposition in the field: A comparison of models, *Ecology*, *68*, 1190–1200, doi:10.2307/1939203.

Antonopoulos, V. S. (1999), Comparison of different models to simulate soil temperature and moisture effects on N mineralization in the soil, *J. Plant Nutr. Soil Sci.*, *162*, 667–675, doi:10.1002/(SICI)1522-2624(199912)162:6<667::AID-JPLN667>3.0.CO;2-D.

Bo, S., and L. Xin-Xiong (1993), Effects of soil texture and $CaCO_3$ on turnover of organic material in Chao soils, *Pedosphere*, *3*, 133–144.

Bosatta, E., and G. I. Agren (1997), Theoretical analyses of soil texture effects on organic matter dynamics, *Soil Biol. Biochem.*, *29*, 1633–1638, doi:10.1016/S0038-0717(97)00086-2.

Bottner, P., and F. Warembourg (1976), Method for simultaneous measurement of total and radioactive carbon in soils, soil extracts and plant materials, *Plant Soil*, *45*, 273–277.

Bottner, P., M. Pansu, L. Sarmiento, D. Hervé, R. Callisaya-Bautista, and K. Metselaar (2006), Factors controlling decomposition of soil organic matter in fallow systems of the high tropical Andes: A field simulation approach using ^{14}C and ^{15}N labelled plant material, *Soil Biol. Biochem.*, *38*, 2162–2177, doi:10.1016/j.soilbio.2006.01.029.

Braakhekke, W. G., and A. M. G. de Bruijn (2007), Modelling decomposition of standard plant material along an altitudinal gradient: A re-analysis of data of Coûteaux et al (2002), *Soil Biol. Biochem.*, *39*, 99–105, doi:10.1016/j.soilbio.2006.06.018.

Brookes, P. C., A. Landman, G. Pruden, and D. S. Jenkinson (1985), Chloroform fumigation and the release of soil nitrogen: A rapid direct extraction method to measure microbial biomass nitrogen in soil, *Soil Biol. Biochem.*, *17*(6), 837–842.

Corstanje, R., and R. M. Lark (2008), On effective linearity of soil process models, *Eur. J. Soil Sci.*, *59*, 990–999, doi:10.1111/j.1365-2389.2008.01046.x.

Coûteaux, M. M., P. Bottner, J. M. Anderson, B. Berg, T. Bolger, P. Casals, J. Romanyà, J. M. Thiéry, and V. R. Vallejo (2001), Decomposition of ^{13}C-labelled standard plant material in a latitudinal transect of European coniferous forests: Differential impact of climate on the decomposition of soil organic matter compartments, *Biogeochemistry*, *54*, 147–170, doi:10.1023/A:1010613524551.

Coûteaux, M. M., L. Sarmiento, P. Bottner, D. Acevedo, and J. M. Thiéry (2002), Decomposition of standard plant material along an altitudinal transect (65–3968 m) in the tropical Andes, *Soil Biol. Biochem.*, *34*, 69–78, doi:10.1016/S0038-0717(01)00155-9.

Dalias, P., J. M. Anderson, P. Bottner, and M. M. Coûteaux (2001), Temperature responses of carbon mineralization in conifer forest soils from different regional climates incubated under standard laboratory conditions, *Global Change Biol.*, *7*, 181–192, doi:10.1046/j.1365-2486.2001.00386.x.

Food and Agriculture Organization, United Nations Educational, Scientific and Cultural Organization, and International Soil Reference and Information Centre (FAO, UNESCO, and ISRIC) (1988), *FAO-UNESCO Soil Map of the World*, revised legend, *World Soil Resour. Rep. 60*, 119 pp., Food and Agric. Org., U.N. Educ., Sci., and Cult. Org., and Int. Soil Ref. and Inf. Cent., Rome.

Feller, C., and M. H. Beare (1997), Physical control of soil organic matter dynamics in the tropics, *Geoderma*, *79*, 69–116, doi:10.1016/S0016-7061(97)00039-6.

Gonzalez-Prieto, S. J., A. Cabaneiro, M. C. Villar, M. Carballas, and T. Carballas (1996), Effect of soil characteristics on N Mineralization capacity in 112 native and agricultural soils, *Biol. Fertil. Soils*, *22*, 252–260, doi:10.1007/BF00382521.

Hansen, S., H. E. Jensen, N. E. Nielsen, and H. Svendsen (1991), Simulation of nitrogen dynamics and biomass production in winter wheat using the Danish simulation model DAISY, *Fert. Res.*, *27*, 245–259, doi:10.1007/BF01051131.

Hassink, J., and A. P. Whitmore (1997), A model of the physical protection of organic matter in soils, *Soil Sci. Soc. Am. J.*, *61*, 131–139.

Jenkinson, D. S. (1990), The turnover of organic carbon and nitrogen in soil, *Philos. Trans. R. Soc. London, Ser. B*, *329*, 361–368, doi:10.1098/rstb.1990.0177.

Joergensen, R. G. (1996), The fumigation-extraction method to estimate soil microbial biomass: Calibration of the k (EC) value, *Soil Biol. Biochem.*, *28*, 25–31.

Kätterer, T., M. Reichstein, O. Andrén, and A. Lomander (1998), Temperature dependence of organic matter decomposition: A critical review using literature data analyzed with different models, *Biol. Fertil. Soils*, *27*, 258–262, doi:10.1007/s003740050430.

Ladd, J. N., L. Jocteur-Monrozier, and M. Amato (1992), Carbon turn-over and nitrogen transformation in an Alfisol and Vertisol amended with [U-^{14}C] glucose and [^{15}N] ammonium sulfate, *Soil Biol. Biochem.*, *24*, 359–371, doi:10.1016/0038-0717(92)90196-5.

Ladd, J. N., M. Amato, P. R. Grace, and J. A. van Veen (1995), Simulation of ^{14}C turnover through the microbial biomass in soils incubated with ^{14}C-labelled plant residues, *Soil Biol. Biochem.*, *27*, 777–783, doi:10.1016/0038-0717(94)00243-T.

Leirós, M. C., C. Trasar-Cepeda, S. Seoane, and F. Gil-Sotres (1999), Dependance of mineralisation of soil organic matter on temperature and moisture, *Soil Biol. Biochem.*, *31*, 327–335, doi:10.1016/S0038-0717(98)00129-1.

Lomander, A., T. Kätterer, and O. Andrén (1998), Modelling the effects of temperature and moisture on CO_2 evolution from top- and subsoil using a multi-compartment approach, *Soil Biol. Biochem.*, *30*, 2023–2030, doi:10.1016/S0038-0717(98)00077-7.

Ma, L., and M. J. Shaffer (2001), A review of carbon and nitrogen processes in nine U.S. soil nitrogen dynamics models, in *Modelling Carbon and Nitrogen Dynamics for Soil Management*, edited by M. J. Shaffer, L. Ma, and S. Hansen, pp. 55–102, Lewis Publ., Boca Raton, Fla.

Manzoni, S., and A. Porporato (2007), A theoretical analysis of nonlinearities and feedbacks in soil carbon and nitrogen cycles, *Soil Biol. Biochem.*, *39*, 1542–1556, doi:10.1016/j.soilbio.2007.01.006.

Manzoni, S., and A. Porporato (2009), Soil carbon and nitrogen mineralization: Theory and models across scales, *Soil Biol. Biochem.*, *41*(7), 1355–1377.

Martin, J. P., and K. Haider (1986), Influence of mineral colloïds in turn-over rates of soil organic carbon, in *Interactions of Soil Minerals With Organics and Microbes*, edited by P. M. Huang and M. Schnitzer, pp. 283–304, Soil Sci. Soc. Am., Madison, Wisc.

McGechan, M. B., and L. Wu (2001), A review of carbon and nitrogen processes in European soil nitrogen dynamics models, in *Modelling Carbon and Nitrogen Dynamics for Soil Management*, edited by M. J. Shaffer, L. Ma, and S. Hansen, pp. 103–171, Lewis Publ., Boca Raton, Fla.

Mueller, T., L. S. Jensen, J. Magid, and N. E. Nielsen (1997), Temporal variation of C and N turnover in soil after oilseed rape straw incorporation in the field: Simulations with the soil-plant-atmosphere model DAISY, *Ecol. Modell.*, *99*, 247–262, doi:10.1016/S0304-3800(97)01959-5.

Pansu, M., J. Gautheyrou, and J. Y. Loyer (2001), *Soil Analysis: Sampling, Instrumentation and Quality Control*, A.A. Balkema, Lisse, Netherlands.

Pansu, M., P. Bottner, L. Sarmiento, and K. Metselaar (2004), Comparison of five soil organic matter decomposition models using data from a ^{14}C and ^{15}N labeling field experiment, *Global Biogeochem. Cycles*, *18*, GB4022, doi:10.1029/2004GB002230.

Pansu, M., L. Sarmiento, K. Metselaar, D. Hervé, and P. Bottner (2007), Modelling the transformations and sequestration of soil organic matter in two contrasting ecosystems of the Andes, *Eur. J. Soil Sci.*, *58*, 775–785, doi:10.1111/j.1365-2389.2006.00867.x.

Pansu, M., Y. Martineau, and B. Saugier (2009), A modelling method to quantify in situ the input of carbon from roots and the resulting C turnover in soil, *Plant Soil*, *317*(1), 103–120, doi:10.1007/s11104-008-9791-1.

Parton, W. J., D. S. Schimel, C. V. Cole, and D. S. Ojima (1987), Analysis of factors controlling soil organic matter levels in Great Plains grasslands, *Soil Sci. Soc. Am. J.*, *51*, 1173–1179.

Penning de Vries, F., D. Jansen, H. ten Berge, and A. Balkema (1989), *Simulation of Ecophysiological Processes and Growth in Several Annual Crops*, Pudoc, Wageningen, Netherlands.

Percival, H. J., R. L. Parfitt, and N. O. Scott (2000), Factors controlling soil carbon levels in New Zealand grasslands: Is clay content important?, *Soil Sci. Soc. Am. J.*, *64*, 1623–1630.

Poulenard, J., P. Podwojewski, and A. J. Herbillon (2003), Characteristics of non-allophanic Andisols with hydric properties from the Ecuadorian paramos, *Geoderma*, *117*, 267–281, doi:10.1016/S0016-7061(03)00128-9.

Rey, A., C. Petsikos, P. G. Jarvis, and J. Grace (2005), Effect of temperature and moisture on rates of carbon mineralization in a Mediterranean oak forest soil under controlled and field conditions, *Eur. J. Soil Sci.*, *56*, 589–599, doi:10.1111/j.1365-2389.2004.00699.x.

Rodrigo, A., S. Recous, C. Neel, and B. Mary (1997), Modelling temperature and moisture effects on C-N transformations in soils: Comparison of nine models, *Ecol. Modell.*, *102*, 325–339, doi:10.1016/S0304-3800(97)00067-7.

Saggar, S., K. R. Tate, C. W. Feltham, C. W. Childs, and A. Parshotam (1994), Carbon turnover in a range of allophanic soils amended with C-14-labelled glucose, *Soil Biol. Biochem.*, *26*, 1263–1271, doi:10.1016/0038-0717(94)90152-X.

Saggar, S., A. Parshotam, G. P. Sparling, C. W. Feltham, and P. B. S. Hart (1996), ^{14}C-labelled ryegrass turnover and residence times in soils varying in clay content and mineralogy, *Soil Biol. Biochem.*, *28*, 1677–1686, doi:10.1016/S0038-0717(96)00250-7.

Saggar, S., A. Parshotam, C. Hedley, and G. Salt (1999), ^{14}C-labelled glucose turnover in New Zealand soils, *Soil Biol. Biochem.*, *31*, 2025–2037, doi:10.1016/S0038-0717(99)00126-1.

Sarmiento, L., and P. Bottner (2002), Carbon and nitrogen dynamics in two soils with different fallow times in the high tropical Andes: Indications for fertility restoration, *Appl. Soil Ecol.*, *553*, 1–11.

Schjønning, P., I. K. Thomsen, J. P. Møberg, H. de Jonge, K. Kristensen, and B. T. Christensen (1999), Turnover of organic matter in differently textured soils: I. Physical characteristics of structurally disturbed and intact soils, *Geoderma*, *89*, 177–198, doi:10.1016/S0016-7061(98)00083-4.

Smith, P., et al. (1997), A comparison of the performance of nine soil organic matter models using datasets from seven long-term experiments, *Geoderma*, *81*, 153–225, doi:10.1016/S0016-7061(97)00087-6.

Sørensen, L. H. (1981), Carbon-nitrogen relationships during the humification of cellulose in soils containing different amounts of clay, *Soil Biol. Biochem.*, *13*, 313–321, doi:10.1016/0038-0717(81)90068-7.

Thomsen, I. K., P. Schjønning, B. Jensen, K. Kristensen, and B. T. Christensen (1999), Turnover of organic matter in differently textured soils. II. Microbial activity as influenced by soil water regimes, *Geoderma*, *89*, 199–218, doi:10.1016/S0016-7061(98)00084-6.

Thuriès, L., M. Pansu, C. Feller, P. Herrmann, and J. C. Rémy (2001), Kinetics of added organic matter decomposition in a Mediterranean sandy soil, *Soil Biol. Biochem.*, *33*, 997–1010, doi:10.1016/S0038-0717(01)00003-7.

Thuriès, L., M. Pansu, M. C. Larré-Larrouy, and C. Feller (2002), Biochemical composition and mineralization kinetics of organic inputs in a sandy soil, *Soil Biol. Biochem.*, *34*, 239–250, doi:10.1016/S0038-0717(01)00178-X.

van der Linden, A. M. A., J. A. van Veen, and M. J. Frissel (1987), Modelling soil organic matter levels after long-term applications of crop residues, and farmyard and green manures, *Plant Soil*, *101*, 21–28, doi:10.1007/BF02371026.

van Veen, J. A., J. N. Ladd, and M. Amato (1985), Turnover of carbon and nitrogen through the microbial biomass in a sandy loam and a clay soil incubated with [^{14}C(U)]glucose and [^{15}N] $(NH_4)_2SO_4$ under different moisture regimes, *Soil Biol. Biochem.*, *17*, 747–756, doi:10.1016/0038-0717(85)90128-2.

Wang, W. J., C. J. Smith, and D. Chen (2004), Predicting soil nitrogen mineralization dynamics with a modified double exponential model, *Soil Sci. Soc. Am. J.*, *68*, 1256–1265.

Wutzler, T., and M. Reichstein (2008), Colimitation of decomposition by substrate and decomposers: A comparison of model formulations, *Biogeosciences*, *5*, 749–759.

M. Ablan and M. A. Rujano, CESIMO, Facultad de Ingeniería, Universidad de Los Andes, Mérida 5101, Venezuela.

D. Acevedo and L. Sarmiento, ICAE, Facultad de Ciencias, Universidad de Los Andes, Mérida 5101, Venezuela.

M. Pansu, IRD, UMR Eco&Sols, INRA, CIRAD, SupAgro, Université Montpellier, BP 64501, F-34394, Montpellier CEDEX 05, France. (marc.pansu@ird.fr)